

Natural variability of surface oceanographic conditions in the offshore Gulf of Mexico



Frank E. Muller-Karger ^{a,*}, Joseph P. Smith ^b, Sandra Werner ^b, Robert Chen ^a, Mitchell Roffer ^c, Yanyun Liu ^{d,g}, Barbara Muhling ^{d,e}, David Lindo-Atichati ^d, John Lamkin ^e, Sergio Cerdeira-Estrada ^f, David B. Enfield ^d

^aCollege of Marine Science, University of South Florida, St. Petersburg, FL, USA

^bExxonMobil Upstream Research Company, Houston, TX, USA

^cRoffer's Ocean Fish Forecasting Service (ROFFSTM), Melbourne, FL 32904, USA

^dUniversity of Miami, Cooperative Institute for Marine and Atmospheric Studies, Miami, FL 33149, USA

^eNational Oceanic and Atmospheric Administration, Southeast Fisheries Science Center, Miami, FL 33149, USA

^fComisión Nacional para el Conocimiento y Uso de la Biodiversidad (CONABIO), Mexico City, DF, Mexico

^gAtlantic Oceanographic and Meteorological Laboratory, NOAA, Miami, FL, USA

ARTICLE INFO

Article history:

Received 9 August 2014

Received in revised form 25 October 2014

Accepted 8 December 2014

Available online 29 December 2014

ABSTRACT

This work characterizes patterns of temporal variability in surface waters of the central Gulf of Mexico. We examine remote-sensing based observations of sea surface temperature (SST), wind speed, sea surface height anomaly (SSHA), chlorophyll-*a* concentration (Chl-*a*) and Net Primary Production (NPP), along with model predictions of mixed layer depth (MLD), to determine seasonal changes and long-term trends in the central Gulf of Mexico between the early 1980s and 2012. Specifically, we examine variability in four quadrants of the Gulf of Mexico (water depth >1000 m). All variables show strong seasonality. Chl-*a* and NPP show positive anomalies in response to short-term increases in wind speed and to cold temperature events. The depth of the mixed layer (MLD) directly and significantly affects primary productivity throughout the region. This relationship is sufficiently robust to enable real-time estimates of MLD based on satellite-based estimates of NPP. Over the past 15–20 years, SST, wind speed, and SSHA show a statistically significant, gradual increase. However, Chl-*a* and NPP show no significant trends over this period. There has also been no trend in the MLD in the Gulf of Mexico interior. The positive long-term trend in wind speed and SST anomalies is consistent with the warming phase of the Atlantic Multidecadal Oscillation (AMO) that started in the mid-90s. This also coincides with a negative trend in the El Niño/Southern Oscillation Multivariate ENSO Index (MEI) related to an increase in the frequency of cooler ENSO events since 1999–2000. The results suggest that over decadal scales, increasing temperature, wind speed, and mesoscale ocean activity have offsetting effects on the MLD. The lack of a trend in MLD anomalies over the past 20 years explains the lack of long-term changes in chlorophyll concentration and productivity over this period in the Gulf. Understanding the background of seasonal and long-term variability in these ocean characteristics is important to interpret changes in ocean health due to episodic natural and anthropogenic events and long term climate changes or development activities. With this analysis we provide a baseline against which such changes can be measured.

© 2014 The Authors. Published by Elsevier Ltd. Open access under CC BY-NC-ND license.

Introduction

The Gulf of Mexico (Fig. 1) is an area of great economic importance for the United States, Mexico, and Cuba (Adams et al., 2004). It forms part of the circulation of the Atlantic Ocean, serving as a

thruway for the transport of heat, salt and nutrients, and biological material from the Caribbean Sea to the North Atlantic. Thus, it plays a significant role in defining the weather and climate of Central America, the United States, and the Caribbean Sea. It represents important habitat for pelagic fish, marine mammals, and other organisms. A unique geography, rich biodiversity, and high productivity are the foundations for major fisheries and tourism industries in the Gulf of Mexico. This is also an area that has led the world in extensive oil and gas development in deep ocean waters (>300 m) since the 1970s.

* Corresponding author. Address: College of Marine Science, University of South Florida, 140 7[th] Avenue South, St. Petersburg, FL, USA. Tel.: +1 727 553 3335.

E-mail address: carib@usf.edu (F.E. Muller-Karger).

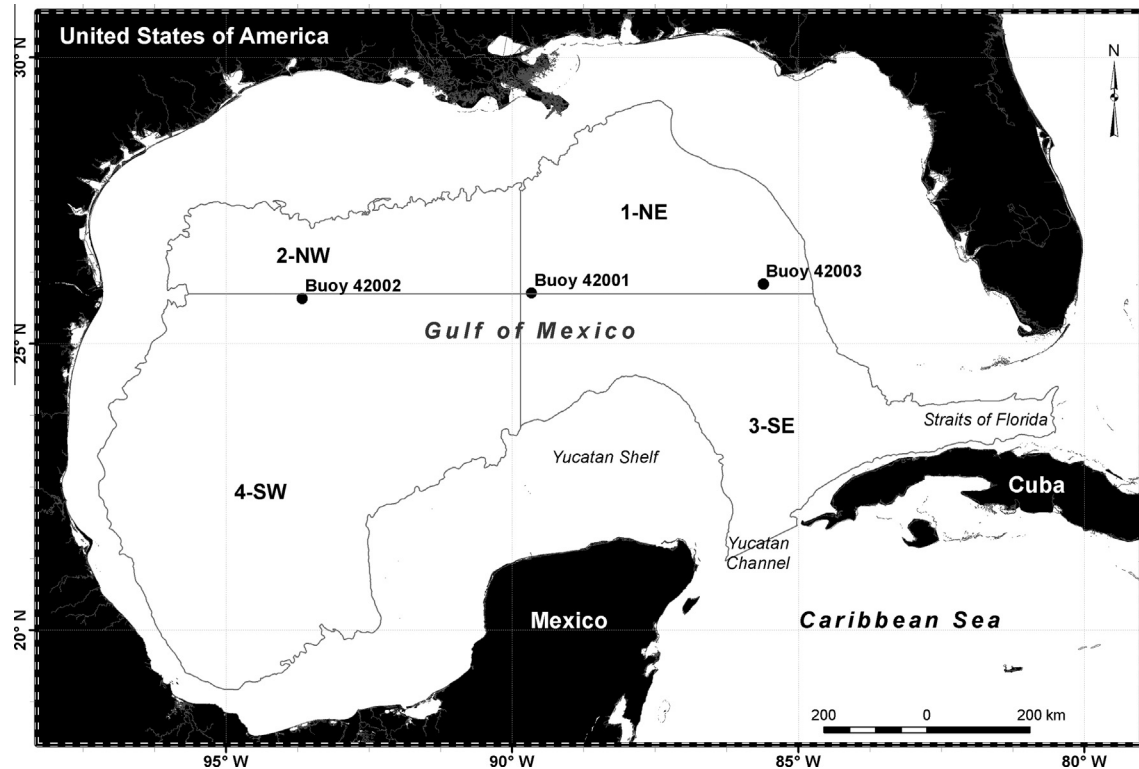


Fig. 1. The Gulf of Mexico. Image shows the four regions of interest (ROI) used to develop the climatological analyses of wind, sea surface temperature, and chlorophyll-a concentration. ROIs referenced in the text are labeled in this figure as 1-NE, 2-NW, 3-SE, and 4-SW. The locations of the NOAA NDBC buoys used for wind data are marked by filled squares; each buoy location is labeled with the NDBC buoy number.

Over the past 60 years we have developed substantial knowledge about the hydrography, circulation, biogeochemical, and biological processes of surface waters of the Gulf of Mexico (e.g. Capurro and Reid, 1972; Muller-Karger et al., 1991; Felder and Camp, 2012; and numerous other publications). This knowledge is based on observations collected by ships, moored instruments, drifting buoys, satellite-based sensors, and numerical simulations. In this paper we present an updated synthesis of the major characteristics of oceanic surface waters in the central Gulf of Mexico. Our study was guided by the objective of testing the hypothesis that the surface waters of the interior Gulf of Mexico, i.e. those seaward of the shelf break, have experienced significant unidirectional change over the past 30 years in a number of oceanographic parameters. Detecting and quantifying such change in large oceanic ecosystems is fundamental to define proper resource use management strategies (Muller-Karger et al., 2014). Our question arose from general interest on how the Gulf of Mexico is behaving in light of the average +0.13 °C per decade increase in sea surface temperature observed over the global ocean since 1979 (Trenberth et al., 2007), or the much higher rates of +0.5 °C per decade observed in the past 20 years over the central Caribbean Sea and the tropical western north Atlantic Ocean (Chollett et al., 2012). Muhling et al. (2012) found that sea surface temperature (SST) in the northern Gulf of Mexico rose about 0.5 °C between 1985 and 2008. They detected a concurrent increase in pelagic fish larvae over the outer continental shelf, with warmer years showing higher abundances of larvae. Muhling et al. (2012) concluded that long-term changes in physical habitat are having important ecological implications in the deep Gulf of Mexico.

Here we focused specifically on key surface ocean properties of the interior of the Gulf of Mexico where the seafloor is deeper than 1000 m. We wanted to understand long-term change in waters

away from the more direct influence of winds and atmospheric temperatures associated with adjacent land, which strongly affect coastal and shelf waters of the Gulf (Muller-Karger, 2000; Zavala-Hidalgo et al., 2003; Morey et al., 2005; Weisberg et al., 1996, 2005). Surface waters of the Gulf of Mexico cover approximately $1.6 \times 10^6 \text{ km}^2$, with waters deeper than the continental shelf covering about $8.6 \times 10^5 \text{ km}^2$. Satellite sensors facilitate the observation of such large areas. We examined the variability of SST, wind speed, sea surface height anomaly (SSHA), mixed layer depth (MLD), chlorophyll-a concentration, and primary productivity in these offshore Gulf of Mexico waters. We sought to quantify oceanographic change over seasonal to decadal timescales and put these variations in the context of decadal-scale change. The need for such information is recognized, especially after the Deepwater Horizon oil spill (e.g. National Ocean Service, 2011).

Background

There is a large body of scientific literature describing the general circulation of surface waters in the Gulf of Mexico (Nowlin et al., 1968; Behringer et al., 1977; Vukovich, 1988; Fratantoni et al., 1998; Lindo-Atchati et al., 2013, and references therein). The Gulf of Mexico forms part of the western boundary current system of the North Atlantic. Clear and warm surface Caribbean Sea water enters the basin via the Yucatan Current. This water can penetrate as far north as 29°N, reaching the vicinity of the Mississippi River delta in the northern Gulf of Mexico. This current transports water volumes between about 24 Sverdrup (Sv) (Sheinbaum et al., 2002) and 32 Sv (Morrison and Nowlin, 1977; Baringer and Larsen, 2001; others). Many studies have focused on possible links between the volume transport through Yucatan Channel, the extent of penetration of the Loop Current into the Gulf

of Mexico, and the processes of ring shedding (Maul et al., 1985; Candela et al., 2003; Bunge et al., 2002; Oey, 1996; Ezer et al., 2003). Oscillations in the Cayman Sea and the Gulf of Mexico were hypothesized to be connected with time-dependent growth of the Loop Current and its penetration into the northern areas of the Gulf (Maul, 1978). As the current extends to the north, it makes a loop by turning east and south, and carries water out of the Gulf via the Straits of Florida (Vukovich et al., 1979; Hurlbert and Thompson, 1980). The Loop Current penetration displaces an equivalent volume of Gulf water which flows back into the Caribbean Sea approximately below 800 m and in shallower counter-currents found typically on the eastern side of the Yucatan Channel (Bunge et al., 2002; Candela et al. 2003; Rivas et al. 2005; Chérubin et al. 2005). Ocean color satellite imagery shows phytoplankton blooms from the Yucatan Peninsula are often entrained into the Yucatan/Loop Current system and transported north and east into the Gulf of Mexico interior (Muller-Karger et al., 1991). Similarly, the Loop Current often entrains water from the Mississippi River along its northern edge and may carry it out of the Gulf of Mexico via the Straits of Florida (Muller-Karger, 1993; Ortner et al., 1995; Del Castillo et al., 2000, 2001; Hu et al., 2005). The Loop Current shows instabilities around its edge, many of which form cyclonic eddies that may grow as they propagate around its periphery. As these eddies grow, they likely play a role in the process of separation of a section of the Loop Current into a large (200–300 km diameter) anticyclonic eddy (Frantoni et al., 1998).

The process of Loop Current extension and anticyclonic eddy separation is the result of a number of interacting seasonal and stochastic processes (Nowlin et al., 2000; Zavala-Hidalgo et al., 2006). In rare years no separation is observed, but separations can occur even up to three times per year. The period between eddies varies between 0.5 and 18.5 months (Vukovich 2007, 2012; Sturges and Leben, 2000; Leben 2005). The time series of satellite altimetry initiated in 1992 shows anticyclonic eddies shed more frequently between about June and September, but eddies have been shed any month of the year (Alvera-Azcárate et al., 2009; Lindo-Atichati et al., 2013; Cardona and Bracco, 2014). Similar inferences have been made from simulations (Chang and Oey, 2010, 2012, 2013a,b; Nedbor-Gross et al., 2014).

In the eastern Gulf of Mexico, the Loop Current and these large eddies can interact with the continental shelf and lead to enhanced coastal upwelling throughout the region (Muller-Karger, 2000; Weisberg et al., 2004). The large anticyclonic Loop Current eddies typically drift toward the west or west-northwest and reach the Texas–Mexico coastal zone after 2–4 months (Muller-Karger et al., 1991; Lindo-Atichati et al., 2013 and references therein). Immediately after shedding an eddy, the Loop Current retracts to a southern position where waters flow more directly between Yucatan Channel and the Straits of Florida. There is much debate on the physical oceanographic processes at play here. Le Hénaff et al. (2012) suggested that blockage is effected by one or more successive cyclones north of the Loop Current boundary. Mildner et al. (2013) suggested that the recently-shed anticyclonic eddy blocks the flow of the Yucatan Current water toward the north. This remains a “chicken and the egg” problem that will require study outside the scope of this paper.

Many of the studies mentioned above have demonstrated that the bulk properties of the water masses of the upper Gulf of Mexico are determined by interaction of the atmosphere and the ocean over seasonal cycles, by mixing of Loop Current water and large anticyclonic and cyclonic eddies, and by upwelling and mixing of waters along the margins of the basin (Herring, 2010; Vidal et al., 1994, and references therein). Sea surface temperature (SST) in the interior of the Gulf of Mexico undergoes a marked seasonal cycle. Waters gain heat through insolation between April and August, but lose heat between September and March (Ettet,

1983; Cerdeira-Estrada et al., 2005; Chang and Oey, 2010). Heat loss in winter is accelerated by storms and cold-air fronts that stimulate Ekman pumping and wind-driven and convective mixing (Muller-Karger et al., 1991; Melo Gonzalez et al., 2000; Villanueva et al., 2010). Muller-Karger et al. (1991) used SST data from the NOAA Advanced Very High Resolution Radiometer (AVHRR) and the Comprehensive Ocean–Atmosphere Data Set (COADS) to document the seasonal cycle of SST in the interior of the Gulf and its relation to the mixed layer depth. Highest SST of ~29–30 °C occur throughout the interior of the Gulf between July and September. SST minima occur in February–March, with ~22–24 °C observed in the western half of the Gulf, and ~24–26 °C in eastern half where the Loop Current has a direct influence. The density changes associated with temperature and the changes in wind forcing lead to a seasonal cycle in mixed layer depth (MLD), with shallow MLD ~20 m during boreal summers and ~125 m in winter (Muller-Karger et al., 1991).

Even today there are very limited field observations available to characterize how large-scale physical forces have affected the basic biogeochemical characteristics of the interior of the Gulf of Mexico over time. Such inferences have been facilitated by satellite observations. Muller-Karger et al. (1991) examined the spatial and temporal changes in phytoplankton concentrations over the Gulf of Mexico region using synoptic ocean color satellite imagery collected with the NASA Coastal Zone Color Scanner (CZCS; 1978–1986). They found a seasonal variation in phytoplankton concentration seaward of the shelf, with lowest values in May–July (<0.06 mg m⁻³) and high values in December–February (>0.2 mg m⁻³). Winter fronts and storms are particularly frequent during El Niño–Southern Oscillation years (Melo Gonzalez et al., 2000; Kennedy et al., 2007). These storms lead to increased mixing and higher phytoplankton concentrations in the deep Gulf of Mexico during El Niño years (Melo Gonzalez et al., 2000).

Martínez-López and Zavala-Hidalgo (2009) derived a synthetic 12-month climatology of chlorophyll-a concentrations using estimates derived by NASA using the Sea-viewing Wide-Field-of-view Sensor (SeaWiFS) for the period 1997–2007. They found the highest variations in chlorophyll-a concentration on the shelf and along the shelf-break. Using the climatology, they identified complex temporal patterns of wind-driven export of shelf materials to the interior of the Gulf off the Mississippi River Delta, off the Louisiana–Texas shelf, off Veracruz, and in the southern Bay of Campeche. Salmerón-García et al. (2011) also used long-term monthly mean SeaWiFS chlorophyll-a concentration estimates to derive a thematic climatological (1998–2008) classification of Gulf of Mexico biogeographic regions. Callejas-Jimenez et al. (2012) conducted a similar spatial climatological (2002–2007) classification but combining SST, chlorophyll-a, and normalized water-leaving radiance observations derived by NASA using the Moderate Resolution Imaging Spectrometer (MODIS on the Aqua satellite). These studies all reached the conclusion that continental shelf waters (i.e. those where the bottom is shallower than about 200 m) host upwards of a dozen different biogeographic regions distributed around the periphery of the Gulf. Waters seaward of the continental shelf were generally classified as a single biogeographic region, with the caveat that the northeastern and northwestern corners of the Gulf experience seasonal offshore advection of coastal waters (Muller-Karger et al., 1991; Muller-Karger, 2000; Biggs and Muller-Karger, 1993; Biggs et al., 2005; Martínez-López and Zavala-Hidalgo, 2009).

The analysis we present here updates these studies for surface waters over the deep Gulf of Mexico. The study is based on time series of synoptic satellite observations collected from the 1980s through 2012, with more limited observations collected with the Coastal Zone Color Scanner starting in 1978. The observations allow the characterization of the variability in physical parameters that affect the biological production of surface ocean waters.

More specifically, among the physical variables we examined were SST, sea surface height (SSH), wind speed, and MLD. SST is an index of the turbulent and thermodynamic heat flux balance of the surface ocean. It plays a role in determining the rate of metabolic processes within organisms, and is used by biota as a cue for migratory, reproductive, and feeding behavior. Satellite SST observations provide the most comprehensive, long-term records of daily physical variability in the world's ocean. Wind speed contributes to the vertical pumping of nutrients and mixing of biogeochemical properties in the upper layers of the ocean. Wind also contributes to the heat flux balance and gas exchange between the ocean's surface and the atmosphere. SSH is strongly related to circulation patterns and to the internal thermal and salinity structure of the ocean (Rio and Hernandez, 2004). In our region, a higher SSH than normal can be caused by an anticyclonic meso-scale circulation feature, but it can also indicate the presence of a deep layer of warmer than average water. Depending on many factors, such as the vertical stratification and the dynamic processes involved, the relationship between isotherms and the SSH can be estimated from altimeter-derived SSHA, in combination with *in situ* and climatological hydrographic observations. In general, variations in the depth of the main thermocline can be associated with variations in the SSHA field (Willis et al. 2004; Shay et al., 2000). The MLD defines the portion of the water column immediately below the surface within which physical and biogeochemical variables are more or less homogeneous. The MLD is the result of the interaction between surface and upper ocean processes of surface heating and cooling, wind and convective mixing, molecular diffusion and horizontal advection. Thus, the MLD has implications for climate and weather in terms of heat and material exchanges between the atmosphere and the deep ocean. It also has important implications for biota, in terms of light limitation and nutrient availability (Sverdrup, 1953; Ryther and Menzel, 1960; Menzel and Ryther, 1961).

Among biological parameters that serve as an index to the biological state of the Gulf of Mexico we examined Chlorophyll-a (Chl-a) and Net Primary Production (NPP). Chl-a is an index of the standing stock of phytoplankton in ocean waters, typically expressed in units of biomass per unit volume of water. Chl-a also serves as an indicator of vertical mixing of nutrients in the upper ocean and as a tracer of the horizontal dispersal of upwelling or river plumes. Chl-a is typically a small fraction of the particulate organic carbon (POC) in the water (i.e. a few percent). Carbon to Chl-a ratios vary widely (C:Chl-a can range from < 10 to >300 mg C mg Chl-a⁻¹), with lower values typical of diatoms and/or nutrient replete conditions (Yoder, 1979; Laws and Bannister, 1980; Falkowski et al., 1985; Li et al., 2010; and many others). Higher values (>200 mg C mg Chl-a⁻¹) are more typical of non-diatom and/or nutrient limiting conditions. The C:Chl-a ratio also tends to decrease with depth toward the deep Chl-a maximum, below which C:Chl-a may again increase with depth. There still are very few systematic time series measurements of this parameter in the world's ocean. We did not find any published time series of C:Chl-a for the interior of the Gulf of Mexico in waters deeper than the continental shelf edge. In our discussion below we explore the implications of variations in the C:Chl-a with season as related to Chl-a biomass observations from satellite-based sensors.

NPP is a measure of the rate of carbon fixation by phytoplankton (photosynthesis). It is typically expressed as the biomass (in units of weight of carbon) under a square meter of the ocean per unit time. NPP is a complex function of the physiology of phytoplankton, growth rate, C:Chl-a ratios, temperature, nutrient, and sunlight and nutrient history and availability (Cloern et al., 1995; Li et al., 2010).

Time series of NPP and of Chl-a derived from satellites thus provide proxy information on trophic dynamics of surface waters of the ocean that is helpful to study the impact of variations in near-surface water column thermal structure and mixing.

About two decades of synoptic observations of all of these parameters are now available. The phytoplankton pigment concentration time series derived from SeaWiFS (1997–2010) and MODIS-Aqua (2002–2013) provide excellent data with which we can re-examine the inferences made about biological variability based on the CZCS observations collected between 1978 and 1986 (Muller-Karger et al., 1991; Melo Gonzalez et al., 2000). For this purpose we also used a new version of the CZCS dataset, reprocessed by NASA in 2011 using bio-optical algorithms that are consistent with those used by SeaWiFS and MODIS.

We also compared the variability in these observations with common indices of climate variability, in particular the Atlantic Multidecadal Oscillation (AMO; Enfield et al., 2001) and the El Niño/Southern Oscillation Multivariate ENSO Index (ENSO MEI; Wolter and Timlin; 2011). The AMO changed from a warm to cool phase in the mid-60s and from a cool to warm phase in the mid-90s (Enfield and Cid-Serrano 2006, 2010). The Gulf of Mexico ecosystem seems to have shifted in response to this change in the phase of the AMO (Karnauskas et al., 2013). Simulations under various future climate scenarios also suggest that the Loop Current (LC) in the Gulf of Mexico may slow down as part of a deceleration of the Atlantic Meridional Overturning Circulation (AMOC), one of the major mechanisms affecting variability in the AMO (Liu et al., 2012).

With this study we provide a baseline against which such changes can be measured in the Gulf of Mexico. We revisit the conclusions of Muller-Karger et al. (1991) that the seasonal phytoplankton biomass is defined by variations in the mixed layer, and examine how interannual variability in environmental parameters may affect the primary productivity of Gulf waters over decadal scales.

Methods

To test the hypothesis of whether the oceanography of surface waters of the Gulf of Mexico has changed over the past 20+ years, we developed decadal-scale time series of various surface ocean parameters for the Gulf of Mexico based on satellite observations. We divided the Gulf into four quadrants (Fig. 1). Regions of Interest (ROI) were defined as areas between the 1000 m isobath and a point located at 27.78°N, 89.86°W in the central Gulf of Mexico. This point was chosen arbitrarily to divide the Gulf roughly into east, west, north and south. The northern quadrants coincide roughly with the U.S. Exclusive Economic Zone (EEZ). The eastern quadrants represent the area which is influenced by the Loop Current and where the anticyclonic eddy shedding process occurs. We examine variability and trends in wind intensity, sea surface temperature (SST), sea surface height anomaly (SSHA), phytoplankton pigment concentration (chlorophyll-a or Chl-a) and Net Primary Production (NPP) derived from satellite observations for each of these quadrants. Weekly, monthly and annual arithmetic means, and the corresponding long-term means (i.e. "climatologies") were computed for each parameter.

Time series of anomalies of wind speed, SST, SSHA and Chl-a concentration were obtained by subtracting the long-term monthly mean (climatology) from the monthly field for that variable. Anomalies thus represent de-seasoned decadal-scale time series of the corresponding observables. They were used to examine trends using a test for significance of the difference between the slope of the trend derived by least-squares linear regression and a slope of zero. Using

anomalies helped to mitigate the effect of autocorrelation in examining the characteristics of these time series.

Wind (1987–2011)

We used monthly averages (1987–2011) of the Cross-Calibrated, Multi-Platform Ocean Surface Wind Velocity Product (CCMP; [Atlas et al., 2011](#)) available from NASA (ftp://podaac-ftp.jpl.nasa.gov/allData/ccmp/L3.0/docs/ccmp_users_guide.pdf). This ocean surface (10 m) wind product, mapped to a $0.25 \times 0.25^\circ$ degree cylindrical grid, incorporates cross-calibrated satellite winds derived from SSM/I, SSMIS, AMSR-E, TRMM TMI, QuikSCAT, SeaWinds, WindSat, and other satellite instruments. The product is assumed to avoid the diurnal cycle bias that may be expected in observations from single polar-orbiting wind sensors ([Tang et al., 2014](#)). We specifically used scalar wind speed and derived long-term monthly average winds (i.e. a ‘climatology’) to examine anomalies and long-term trends in the winds experienced in the region.

To evaluate the quality of the satellite-derived ocean wind data, wind observations were extracted from three oceanographic buoys maintained in the central Gulf of Mexico since the mid-1970s by the National Oceanic and Atmospheric Administration’s National Data Buoy Center (NOAA NDBC). Specifically, we selected the following NDBC buoys, identified by their number ([Fig. 1](#)):

- Buoy 42001 (25.888°N, 89.658°W; central Gulf; depth of 3365 m; 1975–2012 inclusive).
- Buoy 42002 (25.790°N, 93.666°W; west-central Gulf; 3566 m; 1973–2012 inclusive; note that this buoy was previously positioned at 25.167°N, 94.417°W, about 60 miles to the SW. This change in position is small and does not lead to a change in results).

- Buoy 42003 (26.044°N, 85.612°W; east-central Gulf; 3283 m; 1976–2012 inclusive).

We derived long-term monthly average scalar wind speed from these buoys to compare with the CCMP wind ‘climatology’ mentioned above ([Fig. 2](#)). The buoy data were also used to validate any inferences of long-term trends in wind speed. The buoys were useful to evaluate the representativeness of the CCMP wind statistics for different ROI.

Sea surface temperature (1982–2013)

SST was derived from infrared (IR) observations collected by a number of different satellites. Data were processed at different spatial and temporal resolutions for various tests conducted for our study. Specifically, a time series of daily SST observations spanning 1982–2012 (inclusive) was extracted from the Advanced Very High Resolution Radiometer (AVHRR) Pathfinder Version 5.2 (PFV5.2). The nominal spatial resolution of these data is $4 \times 4 \text{ km}^2$ per pixel. The data were obtained from the US National Oceanographic Data Center (NODC) and the Group for High Resolution Sea Surface Temperature (GHSST) (<http://pathfinder.nodc.noaa.gov>; [Casey et al., 2010](#)). The Pathfinder v5.2 dataset has a gap, from October 2, 1994 to January 17, 1995. This gap was filled for our Gulf of Mexico time series with Local Area Coverage (LAC) AVHRR data collected and processed at the University of South Florida (USF). The daily AVHRR LAC data cover the period August 1993 to 2013. These images were processed at a spatial resolution of approximately $1 \times 1 \text{ km}^2$ per pixel. Likewise, daily data from the MODIS Aqua sensor were processed to estimate SST using the $11 \mu\text{m}$ band at approximately $1 \times 1 \text{ km}^2$ per pixel.

We computed long-term weekly and monthly mean and standard deviation (SD) time series for these datasets by binning all

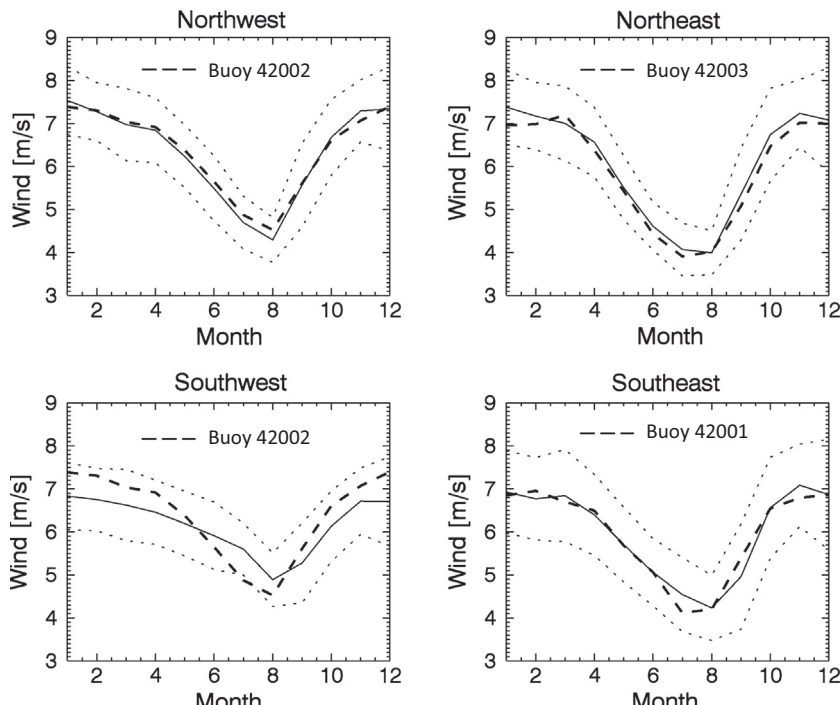


Fig. 2. Wind speed monthly climatology for the four ROI's defined for the interior Gulf of Mexico ([Fig. 1](#)). Regions of Interest: Northeast (upper right), Northwest (upper left), Southeast (lower right), and Southwest (lower left) quadrants ([Fig. 1](#)). Solid curves show the monthly mean climatology (1987–2011) derived from the Cross-Calibrated, Multi-Platform Ocean Surface Wind Velocity Product (CCM). The stippled curves on either side show the mean \pm one standard deviation. The standard deviation was derived on a per pixel basis while constructing the long-term climatological means, and then was averaged over each ROI for each climatological month. The broken line overlaid on each climatological mean wind speed curve is the long-term monthly wind speed means derived from NOAA buoys (Buoy 42001: 1975–2012 inclusive; Buoy 42002: 1973–2012 inclusive; Buoy 42003: 1976–2012 inclusive).

daily night-time only data from each sensor, and for each month across years for each pixel. The Pathfinder v5.2 SST climatology thus is represented by 52 synthetic weekly means and SD, or 12 values for the monthly mean and SD, constructed over the period 1982–2010 (inclusive). The October 1994–January 1995 gap in Pathfinder v5.2 data mentioned above was not filled for purposes of computing the climatology. The MODIS and AVHRR SST monthly climatology (mean and SD) were computed for the period 2003–2010 (inclusive). The choice of years was chosen since it is the period of overlap with SeaWiFS observations.

The Pathfinder v5.2 SST time series for the Gulf of Mexico was compared against the USF AVHRR and MODIS Aqua data. These long-term, night-time SST climatologies were similar in each of the four Gulf of Mexico quadrants (Fig. 3). The similarity provides confidence in the accuracy of the data and in long-term patterns observed with them. In the past, we have found that the various satellite data underestimate *in situ* observations slightly, in the order of about -0.5°C (Hu et al., 2009). In the present study we examined SST anomalies and long-term trends, and therefore ignored this small bias.

Sea surface height anomaly (1992 – 2012)

The sea surface height anomaly (SSHA) is the difference between the best estimate of the sea surface height and a mean sea surface derived from long-term observations from satellite altimeters. This ‘anomaly’ thus preserves seasonal signals. We derived a time series of monthly SSHA estimates for the four Gulf of Mexico quadrants using satellite altimetry observations gridded by the French CNES AVISO office (Archiving, Validation and Interpretation of Satellite Oceanographic data; Le Traon et al., 1998). The altimetric observations used for our time series correspond to Jason-1, TOPEX/Poseidon, The European Remote Sensing (ERS) Satellites 1 and 2, the Environmental Satellite (ENVISAT), and the Geodetic Satellite (GEOSAT) and the GEOSAT Follow-On (GFO), with data starting in October 1992. These interpolated gridded

fields have a spatial resolution of $0.25 \times 0.25^{\circ}$ and temporal resolution of 1 week.

To examine long-term variability in SSHA in the region, we computed long-term monthly mean and standard deviation (SD) of the AVISO datasets (Fig. 4). These climatologies were derived by binning all weekly data. The AVISO SSHA climatology is represented by 12 values for the monthly mean and standard deviation constructed over the period October 1992–December 2012 (inclusive). We also examined the decadal-scale variability and trends in the de-seasoned SSHA (i.e. the monthly SSHA anomaly) as an indicator of mean sea surface elevation change and to assess ocean mesoscale activity.

Because we analyzed climatologies and time series of anomalies, we did not add the mean sea surface elevation to the SSHA fields. The AVISO sea surface height anomaly (SSHA) fields were computed with respect to the 1993–1999 mean from direct altimetry observations.

Mixed layer depth

We sought to derive a time series of monthly mean mixed layer depth estimates for the four offshore Gulf of Mexico quadrants using all *in situ* data holdings of the NOAA National Oceanographic Data Center (NODC). After downloading all ship cast, XBT, drifting buoy, and glider data available at NODC, we found that the data still are insufficient to derive a reasonable time series to cover the period of our study. We therefore did not use these data in this analysis. As an alternative to field measurements for assessment of variability in the mixed layer, we examined daily output fields (1992–2012 inclusive) of the ECCO2 model (ECCO2 is an acronym for *Estimating the Circulation and Climate of the Ocean, Phase II*; results available at: <http://ecco2.jpl.nasa.gov/products/>). ECCO2 is Phase II of the High-Resolution Global-Ocean and Sea-Ice Data Synthesis, sponsored by the NASA Modeling, Analysis, and Prediction (MAP) program (Menemenlis et al., 2005a,b, 2008; Wunsch et al., 2009). The underlying model is the Massachusetts Institute of

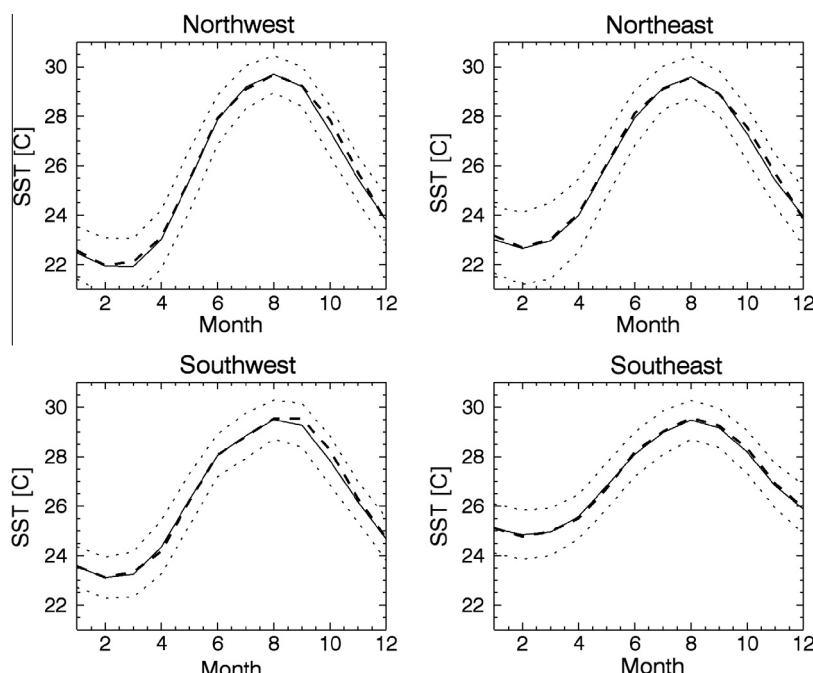


Fig. 3. SST monthly climatology for the four ROI's defined for the interior Gulf of Mexico (Fig. 1) from the night-time NOAA AVHRR Pathfinder v5.2 (solid line; 1982–2010) and the NASA night-time MODIS 11 μm SST product (broken line; 2003–2010). The stippled curves on either side show the mean \pm one standard deviation; the standard deviation were derived from the daily AVHRR Pathfinder v 5.2 SST data, on a per pixel basis while constructing the long-term climatological means, and then these were averaged over each ROI for each climatological month.

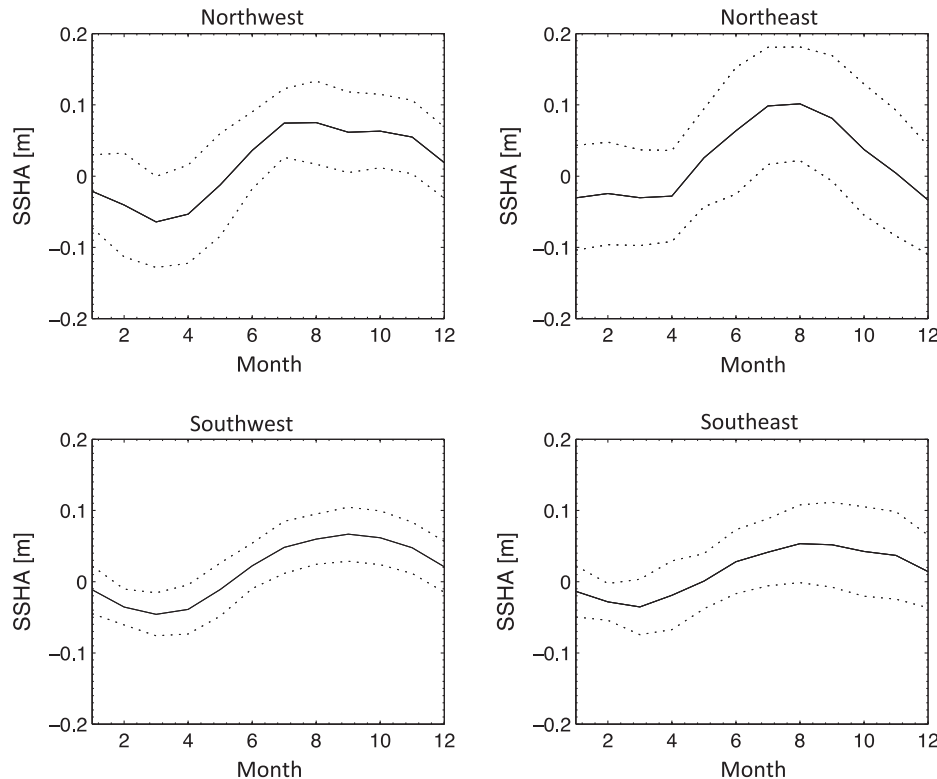


Fig. 4. SSHA monthly climatology for the four ROI's defined for the interior Gulf of Mexico (Fig. 1) from weekly averaged AVISO fields (solid line; 1993–2012 inclusive). The stippled curves on either side show the mean \pm one standard deviation around the long-term monthly SSHA estimates for each region.

Technology general circulation model (MITgcm; Marshall et al., 1997a,b).

ECCO2 is initialized from the World Ocean Database (Conkright et al., 2002) and forced by surface fluxes (wind stress, heat, and freshwater) from the NCEP meteorological synthesis (Kalnay et al., 1996; Kistler et al., 2001). The spatial resolution is 1/4° with 50 vertical levels ranging in thickness from 10 m near the surface to approximately 450 m near the bottom in the deep ocean. The NCEP forcing fields are produced on a 6-hourly basis. Daily average mixed layer depth (MLD) was estimated from the ECCO2 model as the depth at which the potential density relative to the surface is larger than surface density by using the $\Delta\rho = 0.8^\circ\text{C} * \alpha$ criterion, where α is the thermal expansion coefficient at the surface (Kara et al., 2000). Monthly climatologies (Fig. 5) were derived from the time series of daily estimates.

ECCO2 model results in the Gulf of Mexico seem to be realistic and consistent with observations and current understanding of physical oceanographic processes in the region. This includes, for example, the timing and location of shedding of anticyclonic eddies from the Loop Current, vertical flow speeds observed within anticyclonic eddies, and computed Lagrangian Coherent Structures (Lipinski and Mohseni, 2014). Tulloch et al. (2011) also concluded that ECCO2 provided realistic simulations of the Loop Current eddy-shedding process, with the anticyclonic eddies subsequently moving westward in the Gulf. They found that the ECCO2 solutions are in agreement with the simulations of the National Center for Atmospheric Research (NCAR) Climate Community System Model (CCSM; Maltrud et al., 2010).

Chlorophyll-a concentration (mg m^{-3}) and Net Primary Production (NPP; $\text{mg C m}^{-2} \text{ d}^{-1}$) (1978–2013)

In oligotrophic and mesotrophic waters, such as most of the deep Gulf of Mexico, phytoplankton concentration will co-vary

with detritus and colored dissolved organic matter or CDOM concentration (Morel and Prieur, 1977). Under such conditions, ocean color data are an appropriate tool for long term characterization of chlorophyll-*a* variability. Time series of chlorophyll-*a* concentration images of the Gulf of Mexico were derived from data collected by the Coastal Zone Color Scanner (CZCS), the Sea-viewing Wide-Field-of-view Sensor (SeaWiFS), and the Moderate Resolution Imaging Spectrometer (MODIS on NASA's Aqua satellite). The CZCS observations span October 1978 through May 1986, when the sensor stopped working. The SeaWiFS measurements span January 1998 through November 2010. SeaWiFS stopped working in December 2010. We merged the MODIS and SeaWiFS data series for our long-term analyses of chlorophyll concentrations, with SeaWiFS data spanning 1998–2002 (inclusive). MODIS data spanned January 2003–January 2013.

Ocean color data from the CZCS, SeaWiFS, and MODIS Aqua satellite sensors were obtained from the NASA Goddard Space Flight Center. We used the updated CZCS chlorophyll-*a* data (2011 reprocessing by NASA), SeaWiFS (2010 reprocessing), and MODIS (2013 reprocessing). The 2011 CZCS reprocessing used calibration, atmospheric correction, and band-ratio chlorophyll-*a* concentration algorithms similar to those used by SeaWiFS and MODIS to address the problems listed by Gregg et al. (2002). All products followed the latest implementation of the atmospheric correction based on Gordon and Wang (1994), Gordon (1997), and Ding and Gordon (1995). Chlorophyll-*a* concentration from CZCS, SeaWiFS and MODIS was estimated using the NASA OC4 and OC3 band ratio algorithms (O'Reilly et al., 2000). We used the global $4 \times 4 \text{ km}^2$ resolution gridded CZCS and MODIS chlorophyll-*a* fields and the $9 \times 9 \text{ km}^2$ resolution global SeaWiFS products for the basin-scale analyses.

Gregg et al. (2002) list some of the deficiencies of the CZCS relative to the SeaWiFS and MODIS sensors. They analyzed the global CZCS data using a number of improvements relative to the original

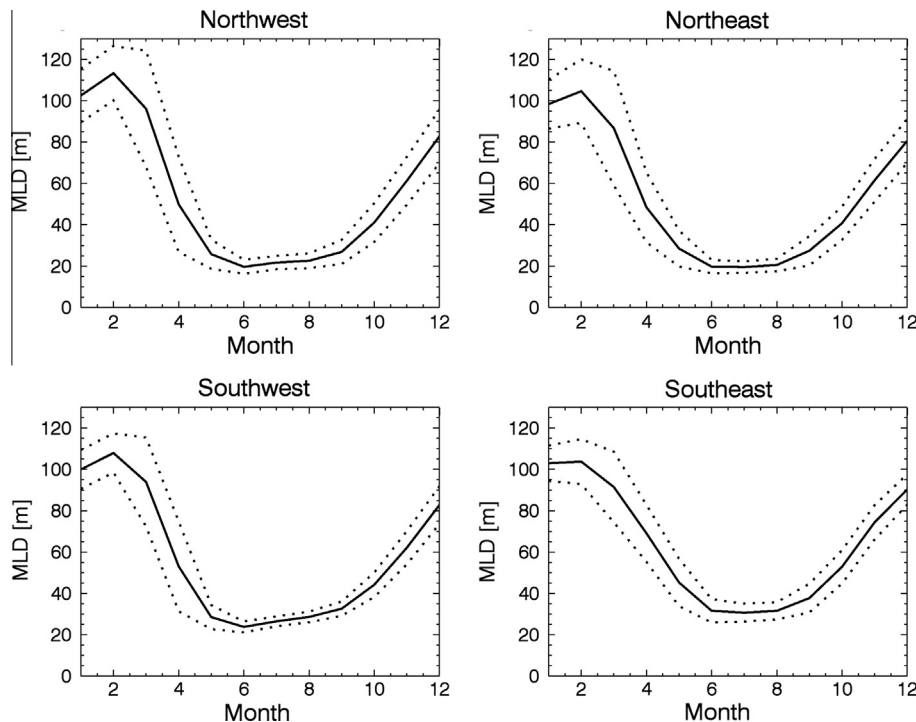


Fig. 5. Mixed layer depth (MLD in meters) monthly climatology derived from daily average ECCO2 simulated MLD fields (1992–2012 inclusive). MLD was derived using the $\Delta\rho = 0.8^{\circ}\text{C} * \text{Alpha}$ criterion, where Alpha is the thermal expansion coefficient at the surface criterion relative to surface temperature. The stippled curves on either side show the mean \pm one standard deviation around the long-term monthly MLD estimates for each region.

CZCS algorithms, including improved calibration and atmospheric correction algorithms. They also applied a 3-band maximum ratio bio-optical algorithm (OC3) intended to estimate chlorophyll-a concentration, as opposed to pigment concentration (the sum of chlorophyll and other pigments). They found that the original CZCS data generally underestimated chlorophyll concentration observations archived by the NOAA National Oceanographic Data Center (NODC) globally by 8–35% (Gregg and Conkright, 2001). On regional and seasonal scales, larger underestimates were common (20–40%, and occasionally the differences exceeded 100%). The reprocessed CZCS data used by Gregg et al. (2002) then led to a slight (~10%) overestimate of global average concentrations. Fig. 6 shows the chlorophyll-a concentration climatologies derived from the three ocean color sensors (CZCS, SeaWiFS, and MODIS). We find that the newly reprocessed CZCS data (2006 NASA reprocessing) overestimates CHL within the subtropics (i.e. not just the Gulf of Mexico) by a factor that can exceed 1.5 during winter. This overestimate of chlorophyll concentrations by CZCS is due to a consistent bias toward lower CZCS remote sensing reflectance at 443 nm (Rrs443) and higher reflectance at 555 nm (Rrs555) relative to SeaWiFS and MODIS. The differences are especially apparent during winter (NASA CZCS Technical Note, 2010).

We attempted to use the CZCS data by applying a bias correction based on a comparison of the CZCS and MODIS monthly mean chlorophyll-a concentration climatology, and subtracting the difference from each CZCS pixel. However, the results (not shown) rendered the CZCS data unusable for any quantitative analysis. The correction effectively forced the CZCS data to look identical to the MODIS imagery on average. In addition to destroying any possible trends in time, it changed the spatial patterns inherent in the Gulf as captured by CZCS imagery. We decided against using such bias correction tools.

Because of our inability to correct the CZCS data, these were not useful for long-term trend analyses. The CZCS data would need to be reprocessed after recalibrating the blue bands using clear water radiance estimates in different hemispheres for each season. The

CZCS data, however, are useful to compare general temporal and spatial patterns observed in the 1980s with those seen with the SeaWiFS and MODIS. This includes, specifically for this study, general seasonal variability in pigment concentration, changes in spatial patterns of ocean color associated with the edges of the Loop Current and eddies, as well as corroborating variability in the seasonal dispersal patterns of Mississippi river water in the Northeastern Gulf of Mexico.

Monthly Net Primary Production (NPP) based on the Vertically Generalized Production Model (VGPM) of Behrenfeld and Falkowski (1997) was computed at $1 \times 1 \text{ km}^2$ spatial resolution from the MODIS Aqua data downloaded from the NASA GSFC. MODIS daily surface chlorophyll-a concentrations, MODIS SST, and MODIS cloud-corrected incident daily photosynthetically active radiation (PAR) at $1 \times 1 \text{ km}^2$ resolution were used as input data. Monthly means for each parameter were used to calculate the weekly and monthly NPP. A monthly climatology (Fig. 7) and a series of monthly anomalies were then derived for each of the quadrants of the Gulf.

Climate indices

Two climate indices commonly used to help explain weather patterns and oceanographic variability were examined to assess whether changes in Gulf of Mexico observables were related to large-scale forcing. Specifically, we used the monthly Atlantic Multidecadal Oscillation (AMO) index of Enfield et al. (2001) and the monthly El Niño/Southern Oscillation Multivariate ENSO Index (ENSO MEI; Wolter and Timlin; 2011). The AMO index is an area-weighted average of the SST estimates over the North Atlantic ($0\text{--}70^{\circ}\text{N}$). It reflects coherent natural variability in the North Atlantic Ocean (Poore et al., 2009). We used the unsmoothed version of the AMO (1948–2013; <http://www.esrl.noaa.gov/psd/data/time-series/AMO/>). The ENSO MEI tracks an ocean–atmosphere coupling that affects variability in climate and weather conditions around the globe.

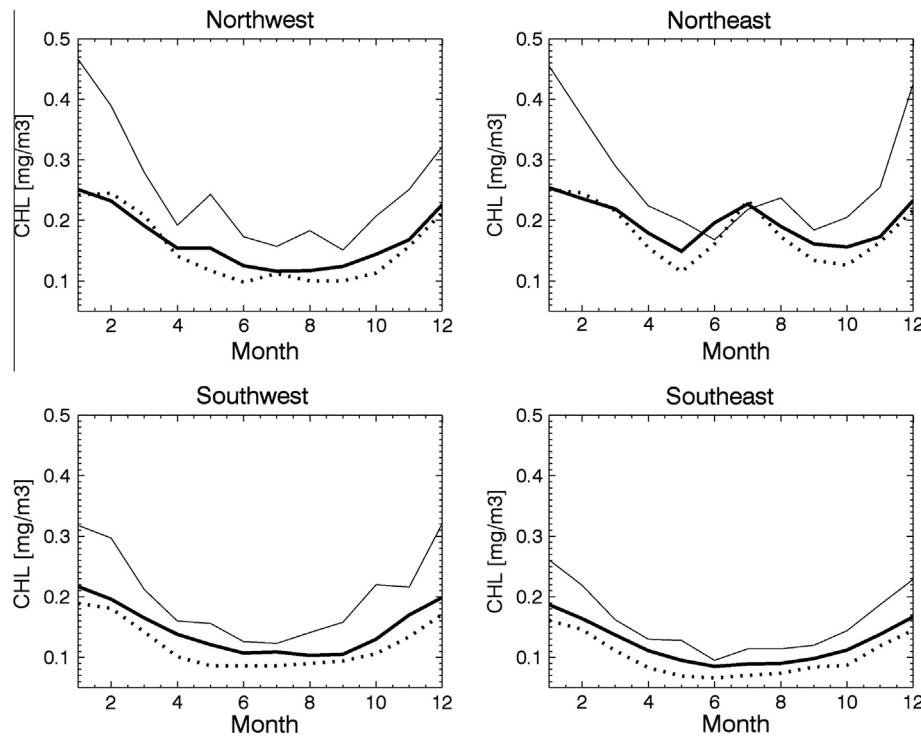


Fig. 6. Chlorophyll-*a* concentration monthly climatology [mg Chl m^{-3}] from four different satellite sensors for the four ROI's defined for the interior Gulf of Mexico (Fig. 1). Thin solid line: CZCS data (1978–1986). Thick solid line: SeaWiFS (1998–2010). Dotted line: MODIS (2003–2010).

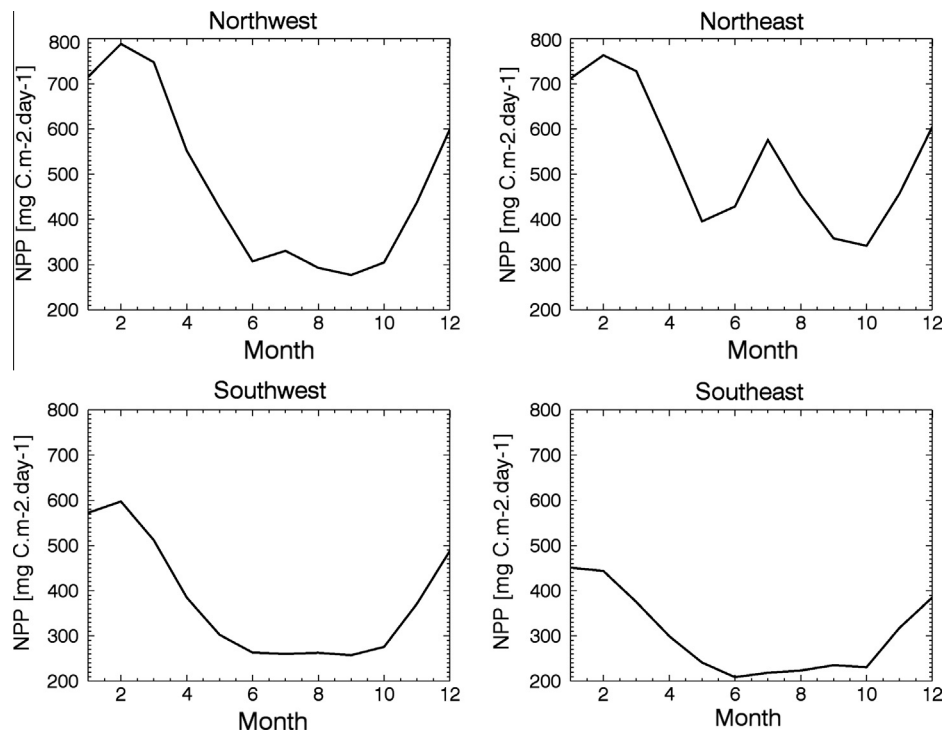


Fig. 7. Net Primary Production climatology (NPP; [$\text{mg C m}^{-2} \text{d}^{-1}$]) derived from MODIS observations (2003–2010) for the four ROI's defined for the interior Gulf of Mexico (Fig. 1).

Results

Wind speed

The long-term monthly average wind intensity derived from the CCM blended product and point measurements at the various NDBC

buoys in the interior of the Gulf of Mexico show a similar seasonal cycle in all four regions, with consistent timing of maxima and minima of the average winds across the entire Gulf of Mexico (Fig. 2). The agreement between the CCMP and buoy wind data show that the CCMP data may be used to examine long-term patterns, including possible trends, in the wind over the Gulf of Mexico.

Different regions showed only slightly different amplitudes in the climatological average wind intensity. They showed similar long-term average maxima in wind intensities of $\sim 7 \text{ m s}^{-1}$ in the November–February timeframe. All areas also showed a decrease in wind intensity from about March–April, and minima (<4 to 5 m s^{-1}) in the July–September timeframe. The minima of this summertime period occur typically in the eastern Gulf of Mexico (winds < 4 m s^{-1} ROI 1 and 3). The standard deviation in the mean monthly wind intensity computed between 1987 and 2011 was similar during November–January compared to July–September periods (i.e. annual range in SD $\sim 0.5\text{--}1.2 \text{ m s}^{-1}$ for all regions).

Fig. 8 shows the monthly wind anomaly in each of the four ROIs. The trend in the anomalies was overlaid on the anomaly curve. All areas show a significant increase in wind intensity with time of the

order of $0.2\text{--}0.3 \text{ m s}^{-1}$ per decade (i.e. the null hypothesis that the slope is zero can be rejected; $p \ll 0.025$). There has been no significant change in wind intensity in summer months (July through September, the period of wind minima). However, over November to January periods, when seasonal winds are highest, winds have strengthened ($>0.36 \text{ m s}^{-1}$ per decade; significant at $p \ll 0.025$) in all areas except the southeastern quadrant of the Gulf of Mexico. In the southeastern quadrant, the increase shows weaker statistical significance. Overall, all regions show an increase in winds of over $>0.72 \text{ m s}^{-1}$ (>1.4 knots) over the last 20 years in winter-time winds. The increase in wind intensity in the Gulf of Mexico region is consistent with the observation that average annual wind intensity has increased gradually over most of the world's ocean area since 1991 (Young et al., 2011a,b).

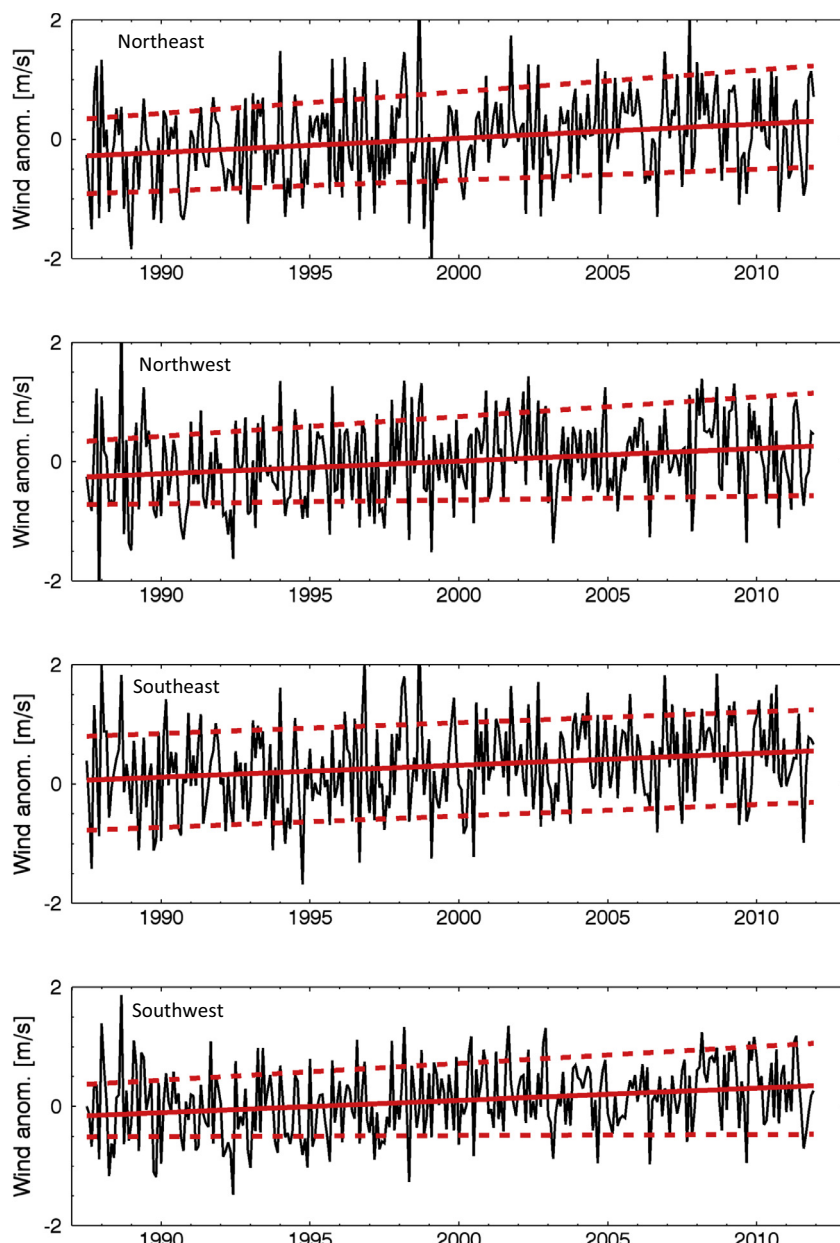


Fig. 8. Wind speed monthly anomaly (1987–2011) relative to the CCM wind climatology for the Gulf of Mexico. From top to bottom, panels show the Northeast, Northwest, Southeast, and Southwest quadrants (Fig. 1). The solid line drawn through the series shows the least squares regression (Nov 1987-Dec 2011) line for the respective ROIs, which has a significant slope of $\sim 0.2 \text{ m s}^{-1}$ per decade for all areas (See Table 1 for statistics). The upper broken line is the least squares regression of wind anomalies for November–January periods, plotted one standard deviation above the mean of the wind intensity anomalies for this period. The lower broken line is the least squares regression for July through September periods, plotted one standard deviation below the mean of the summertime wind intensity anomalies.

Sea surface temperature (SST)

The long-term observations show that the seasonal SST cycle throughout the interior of the Gulf of Mexico is coherent (Fig. 3). All quadrants show minima in February–March and maxima around August. The seasonal SST amplitude change was largest in the western Gulf (~22–23 °C in February–March to ~29–30 °C in August). The SST minima in the southeastern Gulf of Mexico reached only ~24–25 °C. The highest variability in SST is observed during January–March in the northern quadrants of the Gulf.

The time series of monthly regional SST anomalies within each of the quadrants of the Gulf of Mexico shows gradual warming over the period 1982–2012 (Fig. 9). This is consistent with ship- and buoy-based observations of a gradual increase in the average

global upper ocean temperature since the 1870s and especially since the 1960s (Roemmich et al., 2012; Levitus et al., 2001, 2009), and since the mid 1980s in the Caribbean Sea and tropical Atlantic Ocean (Chollett et al., 2012; Scranton et al., 2014) and Gulf of Mexico (Muhling et al., 2012). In the Gulf of Mexico, cooler winters relative to our seasonal climatology were more frequent in the 1980s than in the 2000s. Warmer summers relative to the climatology were also more frequent in the 2000s compared to the 1980s. Indeed, 2009–2012 showed the four warmest consecutive summers of this record of the Gulf, with 2010 and 2011 also showing the coolest winters. On average, all quadrants show a significant ($p < 0.025$) trend of between +0.17 and +0.3 °C per decade (Table 1). The anomalies during August–September periods (when maxima in SST are typically observed) as well as those in

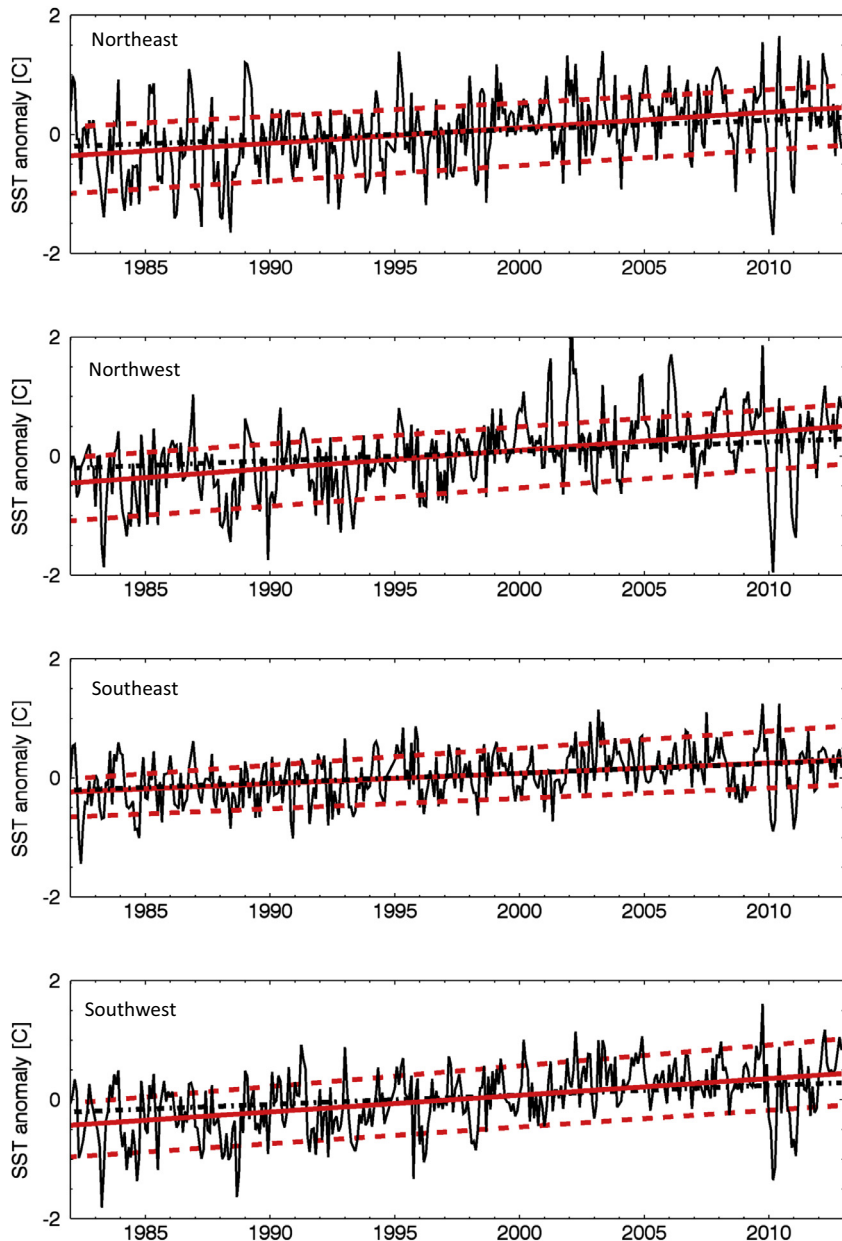


Fig. 9. Monthly SST anomaly (1981–2011) derived relative to Pathfinder SST v5.2 monthly climatology. The least squares regression (November 1981–December 2011) lines are overlaid. All areas showed a slope of between ~0.17 and 0.3 °C per decade (See Table 1 for statistics). The upper broken line is the least squares regression of SST anomalies for August–September periods, plotted one standard deviation above the mean of the SST anomalies for this period. The lower broken line is the least squares regression for February–March periods, plotted one standard deviation below the mean of the wintertime SST anomalies. The broken line overlaid on all graphs is the trendline for the AMO, computed for the period 1981–2012, to overlap with the Pathfinder SST anomaly data.

February–March (months of SST minima) increased at similar rates (significant at $p < 0.025$). The rate of increase in winter temperatures was offset somewhat by the anomalously cold winters of 2010 and 2011, which were especially severe in the northern quadrants. Even though 2010 featured the largest large-scale temperature amplitude variation between winter and summer (i.e. a range $>8^{\circ}\text{C}$ in the southern quadrants and $>9^{\circ}\text{C}$ in northern quadrants) since the beginning of the 1980s, there was no significant trend in the amplitude of the winter–summer SST difference over the observation period. Overall, the highest rates of warming were observed in the northwestern Gulf of Mexico quadrant (i.e. ROI 2; Table 1). Between the 1980s and the decade starting with 2010, this region gained nearly 1°C in average annual SST.

Sea surface height anomaly (SSHA)

Satellite altimetry observations of variations in ocean surface topography provide a measure of heat content, of mesoscale eddy variability, and of the fundamental processes controlling geostrophic ocean currents. Specifically, oceanic pressure centers drive ocean currents much like atmospheric pressure centers drive atmospheric winds. SSHA data also help track changes in ocean heat content on seasonal and longer timescales. In the Gulf of Mexico, the time series of SSHA observations collected since 1992 illustrates and helps quantify the Loop Current ring shedding process when the Loop Current intrudes northward.

The seasonal SSHA cycle in the interior of the Gulf of Mexico is spatially coherent throughout the region (Fig. 4). All quadrants show SSHA minima by late March and SSHA maxima by late August. The seasonal SSHA amplitude was largest in the northern Gulf ($\sim -0.05\text{ m}$ in March to $\sim 0.1\text{ m}$ in August, i.e. an amplitude of 0.15 m) and smallest in the southeastern Gulf ($\sim -0.025\text{ m}$ in March to $\sim 0.025\text{ m}$ in August, i.e. an amplitude of 0.05 m). The signal reflects steric changes due to seasonal warming of the water column, but also the observation that over the course of the satellite altimetry time series, the highest frequency of Loop Current anticyclonic ring-separation events occurred in August and September, with 7 and 4 events, respectively (Lindo-Atchati et al., 2013).

Fig. 10 shows the monthly SSHA anomaly in each of the four ROIs. The trend in the anomalies was overlaid on the anomaly curve. The time series of monthly regional SSHA data within each of the quadrants of the Gulf of Mexico shows a gradual increase in sea level variability over the period 1993–2012. All quadrants show a significant increase of the order of $0.02\text{--}0.03\text{ m}$ per decade. SSHA in the northeastern quadrant is more variable than in the southeastern, northwestern, and southwestern quadrants. This is due to the excursions of the LC into and out of the northeastern region. Also, starting in 2003, the LC was on average located more to the north over the period of our records, and the average number of LC rings formed per year increased (Lindo-Atchati et al., 2013). The increase of SSHA in all quadrants follows the increase of anticyclonic mesoscale activity in the eastern Gulf. The increase in SSHA in the western quadrants is lower than in the eastern quadrants, likely because only part of the warm waters entering the Gulf from the Caribbean are transported to the west. The westward transport of SSHA occurs as the large anticyclonic Loop Current rings migrate in that direction due to a β -plane effect (Shi and Nof, 1994; Nof, 2005). Given the strong relationship that exists between SSHA and the thermal structure of the ocean, our results suggest that the increase in mean SSHA in the interior of the GOM over the last 20 years, which is especially marked since the early 2000s, is linked to the increase in the temperature of the upper water column as shown in the SST observations.

Mixed layer depth (MLD)

The mixed layer depth has an important influence on biological activity in the Gulf of Mexico. The surface mixed layer deepens in winter due to convective mixing and wind forcing, and becomes shallow in summer due to insolation and a weaker seasonal wind regime (Muller-Karger et al., 1991; Melo Gonzalez et al., 2000). The mixing affects the timing and intensity of phytoplankton blooming over large scales, which has important bottom-up ecological implications for fish and other organisms at higher trophic levels (see, for example, Platt et al., 2003; Platt et al., 2007; Muhling et al., 2011).

The ECCO2 simulations show a strong seasonal cycle in the MLD that is of similar magnitude, variability, and phase throughout the interior of the Gulf of Mexico (Fig. 5). All quadrants show MLD maxima of about 90–120 m in February, and minima of about 20 m from about May through October. The southeastern quadrant shows a slightly higher average summer MLD ($\sim 30\text{ m}$). While we have no direct evidence of the causes for this difference, it is possible that the deeper summertime MLD in this region are due to the very warm surface water entering the Gulf from the Caribbean Sea. The upper water column in this sector may be further homogenized by turbulence caused by the interaction between the Yucatan/Loop Current and the continental shelf areas of Yucatan Channel. This affects the average MLD computed over the southeastern region in the $1/4^{\circ}$ spatial resolution model.

The monthly average MLD estimates obtained with the ECCO-2 model for the Gulf of Mexico were similar to the long-term monthly average MLD estimates derived by Muller-Karger et al. (1991) using all NOAA NODC station data collected in Gulf of Mexico waters deeper than 50 m between 1914 and 1985. They are also similar to those provided by a climatological simulation of the region by Ezer (2000). Ezer found that his mixed layer depth simulations were underestimated relative to field observations; he also concluded that his model was rather insensitive to rapid changes in wind speed ($<6\text{ h}$ anomalies of opposite sign). In general, the winter MLD computations based on field data of Muller-Karger et al. (1991; maximum winter MLD of the order of 125–130 m) were slightly larger than those given by ECCO2 (90–120 m). This difference can simply be attributed to a difference in the criterion used to estimate the MLD, among many other factors, and thus cannot be viewed as significant.

There was no evidence of a systematic change in the MLD over time in any of the quarters of the Gulf (Fig. 11). The MLD anomaly showed no noticeable interannual variability during summer months, when the MLD is shallowest. There are some departures from the mean during winter, usually in the range of 20–50 m and short-lived (i.e. one season or shorter). At the beginning of 2010, a strong anomaly was observed during which MLD exceeded 50 m throughout the Gulf of Mexico for several weeks, coinciding with the very cold winter that year.

Chlorophyll-a concentration and Net Primary Production

The chlorophyll-a concentration climatologies derived from each of the three ocean color sensors (CZCS, SeaWiFS, and MODIS) show a clear seasonal pattern that is coherent throughout the deep Gulf of Mexico (Fig. 6). The values and seasonal patterns found in the reprocessed (2011) CZCS data are basically identical to those found by Muller-Karger et al. (1991) using the earlier calibration, atmospheric correction, and bio-optical algorithms from Gordon et al. (1988). The CZCS measurements also show the same seasonal and regional patterns as those from SeaWiFS and MODIS, but the CZCS values are higher by a factor of 1.5 to 2. Because of this, the CZCS data were not used to evaluate changes in phytoplankton chlorophyll concentration between the 1980s and 2000s. The

Table 1

Trends in major satellite-observed parameters based on least-squares linear regression statistics.

Variable	Region of Interest	Climatological monthly mean range [min–max]	Data years [inclusive]	Anomaly trend (overall) [var = A + B * time] (A, B) (R, N) [10 y delta]	Anomaly trend (March–June) [var = A + B * time] (A, B) (R, N) [10 y delta]	Anomaly trend (November–January) [var = A + B * time] (A, B, R, N)
SST (C)	ROI 1	[22.6–29.6]	1981–2012	(A = −52.10, B = 0.026) (R = 0.37, N = 371) [10 y delta = 0.26]	(A = −76.08, B = 0.038) (R = 0.46, N = 124) [10 y delta = 0.38]	(A = −26.96, B = 0.013) (R = 0.22, N = 93) [10 y delta = 0.13]
	ROI 2	[21.9–29.7]	1981–2012	(A = −61.30, B = 0.030) (R = 0.44, N = 371) [10 y delta = 0.31]	(A = −79.6, B = 0.04) (R = 0.50, N = 124) [10 y delta = 0.40]	(A = −38.54, B = 0.019) (R = 0.29, N = 93) [10 y delta = 0.19]
	ROI 3	[24.8–29.5]	1981–2012	(A = −34.73, B = 0.017) (R = 0.37, N = 371) [10 y delta = 0.17]	(A = −44.27, B = 0.022) (R = 0.44, N = 124) [10 y delta = 0.22]	(A = −11.53, B = 0.0) (R = 0.14, N = 93) [10 y delta = 0.05]
	ROI 4	[23.1–29.5]	1981–2012	(A = −56.0, B = 0.028) (R = 0.47, N = 371) [10 y delta = 0.28]	(A = −67.5, B = 0.034) (R = 0.49, N = 124) [10 y delta = 0.34]	(A = −27.87, B = 0.014) (R = 0.30, N = 93) [10 y delta = 0.14]
Wind (m/s)	ROI 1	[4.0–7.4]	1987–2011	(A = −48.83, B = 0.024) (R = 0.24, N = 294) [10 y delta = 0.2]	(A = −40.37, B = 0.020) (R = 0.2, N = 96) [10 y delta = 0.2]	(A = −72.62, B = 0.036) (R = 0.36, N = 74) [10 y delta = 0.4]
	ROI 2	[4.3–7.5]	1987–2011	(A = −43.19, B = 0.022) (R = 0.22, N = 294) [10 y delta = 0.2]	(A = −44.62, B = 0.022) (R = 0.2, N = 96) [10 y delta = 0.2]	(A = −66.07, B = 0.033) (R = 0.34, N = 74) [10 y delta = 0.3]
	ROI 3	[4.2–7.1]	1987–2011	(A = −40.4, B = 0.020) (R = 0.20, N = 294) [10 y delta = 0.2]	(A = −49.7, B = 0.025) (R = 0.25, N = 96) [10 y delta = 0.25]	(A = −35.9, B = 0.02) (R = 0.18, N = 74) [10 y delta = 0.2]
	ROI 4	[4.9–6.3]	1987–2011	(A = −40.7, B = 0.020) (R = 0.25, N = 294) [10 y delta = 0.2]	(A = −58.4, B = 0.029) (R = 0.35, N = 96) [10 y delta = 0.29]	(A = −56.2, B = 0.03) (R = 0.33, N = 74) [10 y delta = 0.3]
SSHA (m)	ROI 1	[−0.03 to 0.1]	1993–2012	(A = −0.03, B = 0.00025), (R = 0.23, N = 238), [10 y delta = 0.03]	(A = −0.006, B = 0.00005), (R = 0.06, N = 238), [10 y delta = 0.006]	(A = −0.01, B = 0.00001), (R = 0.06, N = 238), [10 y delta = 0.01]
	ROI 2	[−0.07 to 0.07]		(A = −0.01, B = 0.00013), (R = 0.16, N = 238), [10 y delta = 0.015]	(A = −0.02, B = 0.0002), (R = 0.23, N = 238), [10 y delta = 0.024]	(A = −0.03, B = 0.00025), (R = 0.28, N = 238), [10 y delta = 0.03]
	ROI 3	[−0.03 to 0.05]		(A = −0.03, B = 0.00013), (R = 0.2, N = 238), [10 y delta = 0.016]	(A = −0.02, B = 0.0001), (R = 0.22, N = 238), [10 y delta = 0.012]	(A = −0.02, B = 0.0002), (R = 0.21, N = 238), [10 y delta = 0.024]
	ROI 4	[−0.04 to 0.06]		(A = −0.02, B = 0.00025), (R = 0.41, N = 238), [10 y delta = 0.2]	(A = −0.03, B = 0.0002), (R = 0.49, N = 238), [10 y delta = 0.024]	(A = −0.02, B = 0.00015), (R = 0.31, N = 238), [10 y delta = 0.018]
Chl-a	ROI 1	CZCS: [0.17–0.46] SeaWiFS/MODIS: [0.12–0.25]	1979–2012	1979–1986: (A = 5.44, B = 0.0, R = 0, N = 88) 2003–2012: (A = 1.27, B = 0.0, R = 0, N = 180) 2009–2013: (A = 58.65, B = −0.03, R = −0.4, N = 49)		
	ROI 2	CZCS: [0.15–0.47] SeaWiFS/MODIS: [0.09–0.25]		1979–1986: (A = 1.0, B = 0.0, R = 0, N = 87) 2003–2012: (A = 0.9, B = 0.0, R = 0, N = 181) 2009–2013: (A = 28.90, B = −0.01, R = −0.3, N = 49)		
	ROI 3	CZCS: [0.10–0.25] SeaWiFS/MODIS: [0.07–0.19]		1979–1986: (A = 6.6, B = 0.0, R = 0.1, N = 90) 2003–2012: (A = 2.0, B = 0.0, R = −0.3, N = 181) 2009–2013: (A = 9.9, B = −0.0, R = −0.3, N = 49)		
	ROI 4	CZCS: [0.12–0.32] SeaWiFS/MODIS: [0.09–0.22]		1979–1986: (A = 12.2, B = 0.0, R = −0.2, N = 90) 2003–2012: (A = 1.2, B = 0.0, R = −0.1, N = 181) 2009–2013: (A = 14.54, B = 0.0, R = −0.3, N = 49)		
MODIS NPP vs. ECCO2 MLD	ROI 1		2003–2012	(A = 5.08, B = 0.09, R = 0.57, N = 121)		
	ROI 2		2003–2012	(A = −9.37, B = 0.14, R = 0.81, N = 121)		
	ROI 3		2003–2012	(A = −19.76, B = 0.28, R = 0.87, N = 121)		
	ROI 4		2003–2012	(A = 22.37, B = 0.22, R = 0.87, N = 121)		

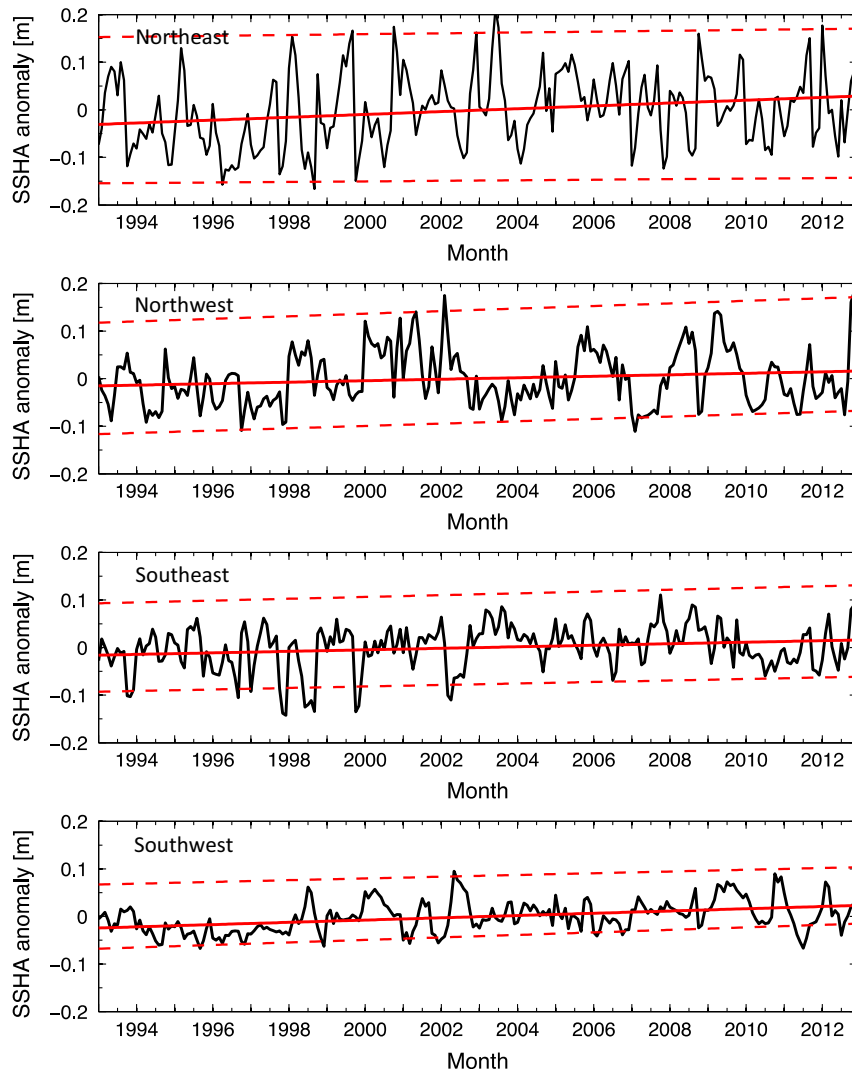


Fig. 10. Monthly SSHA anomaly (1993–2012), derived relative to AVISO SSHA monthly climatology. The least squares regression (January 1993–December 2012) lines are overlaid. All areas showed a slope of between ~ 0.015 and 0.03 m per decade (see Table 1 for statistics). The upper broken line is the least squares regression of SSHA anomalies for August–September periods, plotted one standard deviation above the mean of the SSHA anomalies for this period. The lower broken line is the least squares regression for February–March periods, plotted one standard deviation below the mean of the wintertime SSHA anomalies.

SeaWiFS and MODIS time series, however, show no significant decadal-scale trend in chlorophyll concentration over time in any of the regions of the Gulf (Fig. 12).

Overall, SeaWiFS and MODIS show comparable concentration values throughout the year in all regions, but SeaWiFS tends to overestimate the MODIS data by a few percent during the time of the year when concentrations are very low (<0.15 mg m $^{-3}$), as during April through October. Highest concentrations (0.2–0.25 mg m $^{-3}$) occurred on average in December and January, and minima (<0.1 –0.15 mg m $^{-3}$) in June through September. In general, the CZCS chlorophyll- a data had a significant positive bias (a factor of 1.5–2) relative to SeaWiFS and MODIS.

The two northern Gulf quadrants showed higher concentrations and higher variability compared to the southern quadrants throughout the year. Chlorophyll- a concentrations in both the northwestern and northeastern quadrants show secondary peaks in the monthly climatology. In the northwestern Gulf of Mexico, a small regional peak occurs in May as a result of offshore transport of shelf waters. This is caused by the seasonal convergence of waters coming from the Louisiana-Texas shelf in a counterclockwise direction and from Mexico in a clockwise direction (Zavala-Hidalgo et al. 2003; Martínez-López and Zavala-Hidalgo, 2009;

and Salmerón-García et al., 2011). This peak was particularly conspicuous in the CZCS data, but it is still not clear whether this is simply an issue with the CZCS calibration and distortion of the estimated pigment concentrations.

In the northeastern quadrant, the secondary peak (~ 0.25 mg m $^{-3}$) observed in July in the SeaWiFS and MODIS data, and in August in the CZCS data (also higher values than SeaWiFS and MODIS), represents the offshore (east- and southeastward) dispersal of Mississippi River and other coastal waters from Mississippi and Alabama (Muller-Karger et al., 1991; Gilbes et al., 1996; Morey et al., 2005). We expected to see more variability in this phenomenon, but instead it showed a strong seasonality, occurring in 1982 and 1984 (CZCS) and in 1998, 1999, 2000, 2001, 2003, 2004, 2007, 2008, 2009, 2010, and 2011 (SeaWiFS and MODIS). During the CZCS years, this event was most pronounced in August (1979–1985). In the SeaWiFS and MODIS record, this was strongest in July. The timing of this phenomenon is associated with changes in wind direction and intensity that cause offshore transport to the east and south (D'Sa and Korobkin, 2009; Salisbury et al., 2004; Muller-Karger, 2000). Once off the shelf, the plume can become entrained in the Loop Current or its eddies (Muller-Karger et al., 1991; Del Castillo et al., 2000, 2001; Hu et al., 2005; Martínez-

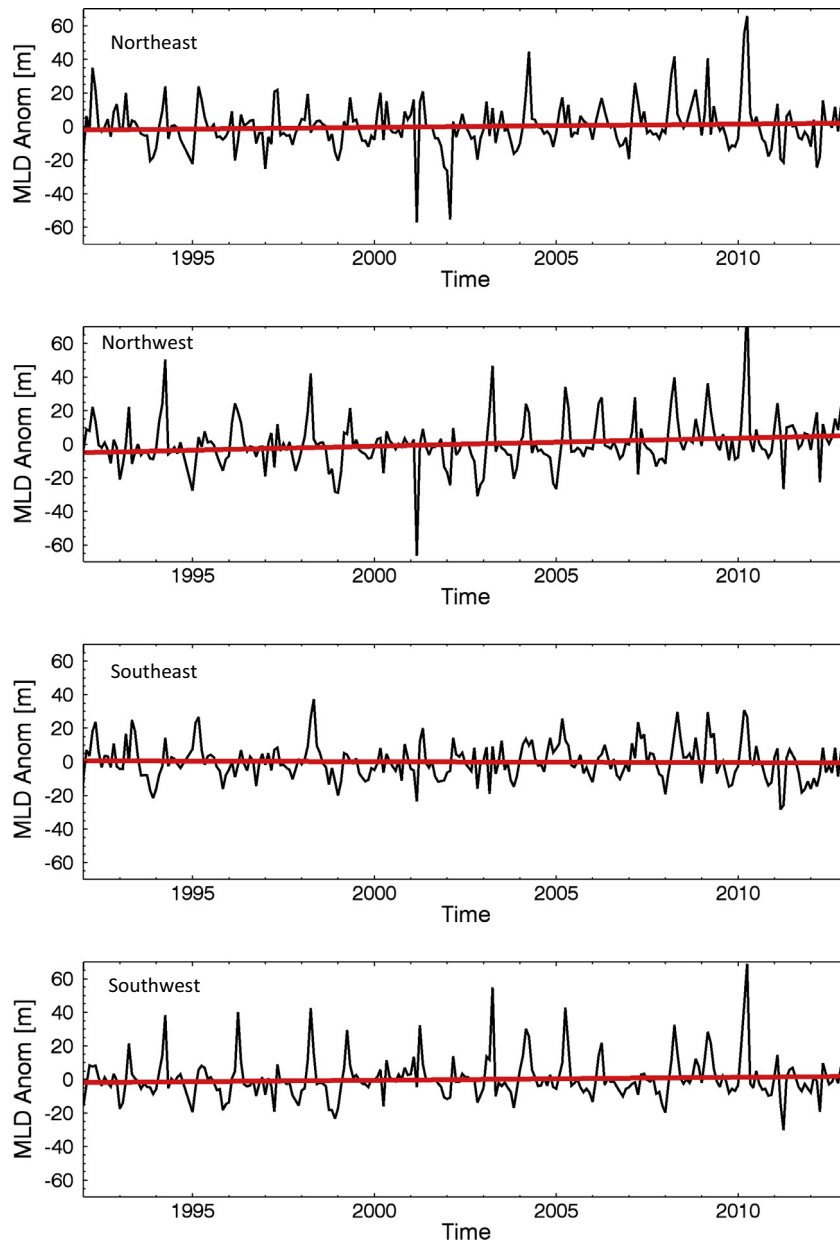


Fig. 11. ECCO2 simulated mixed layer depth anomaly series (m). The least squares regression (January 1992–December 2012) lines are overlaid.

López and Zavala-Hidalgo, 2009). These offshore transports of coastal and shelf waters were especially marked in 1998, 2000, 2008, 2009, and 2010.

To understand how the phytoplankton carbon to Chl-*a* ratio (C:Chl-*a*) may have changed with season, we explored possible ranges in C:Chl-*a* ratios using the model of Cloern et al. (1995). Since there are no published time series of either C:Chl-*a* or of growth rates for the offshore Gulf of Mexico, we assumed possible growth rates in the range of ($\mu =$) 0.2 and 1.0 d⁻¹, SST extremes of 22 and 30 °C, and nominal photosynthetically-active-radiation (PAR; i.e. “irradiance” in the Cloern model) of 1–12 mol quanta m⁻² d⁻¹ in applying the model. Results show that there is likely a seasonality in C:Chl-*a* that coincides with that of Chl-*a*. Estimated C:Chl-*a* of ~3 to 30 mg C (mg Chl-*a*)⁻¹ were estimated for boreal summer (high temperatures and high irradiance, under high or low growth rates). Higher C:Chl-*a* of about 5 to 42 mg C (mg Chl-*a*)⁻¹ were estimated for winter (low temperatures and low irradiance, under high or low growth rates).

The Net Primary Production (NPP) climatology for all four regions (Fig. 7) shows a peak in average productivity in February, i.e. one to two months after the highest chlorophyll values are observed in all quadrants of the Gulf. Values of 700–800 mg C m⁻² d⁻¹ are observed during this time in the northern quadrants of the Gulf. In the southwestern quadrant, the NPP peak is of the order of 600 mg C m⁻² d⁻¹, while it does not exceed 450 mg C m⁻² d⁻¹ in the southeastern quadrant. In all quadrants, the NPP peak occurs during the period of strongest winds (November to February; Fig. 2), and SST minima (Fig. 3), which is when the maximum MLD occurs (Fig. 5). NPP minima in the northern half of the Gulf (300–350 mg C m⁻² d⁻¹) are reached in May. The NPP minimum occurred when the MLD reached its lowest values. Low NPP was maintained while the MLD was shallow, through October (Fig. 5). The southwestern Gulf showed lower values (~250 mg C m⁻² d⁻¹) throughout this period. The lowest average values (~200 mg C m⁻² d⁻¹) occurred in the southeastern quadrant. The NPP minimum period in general coincided with minima

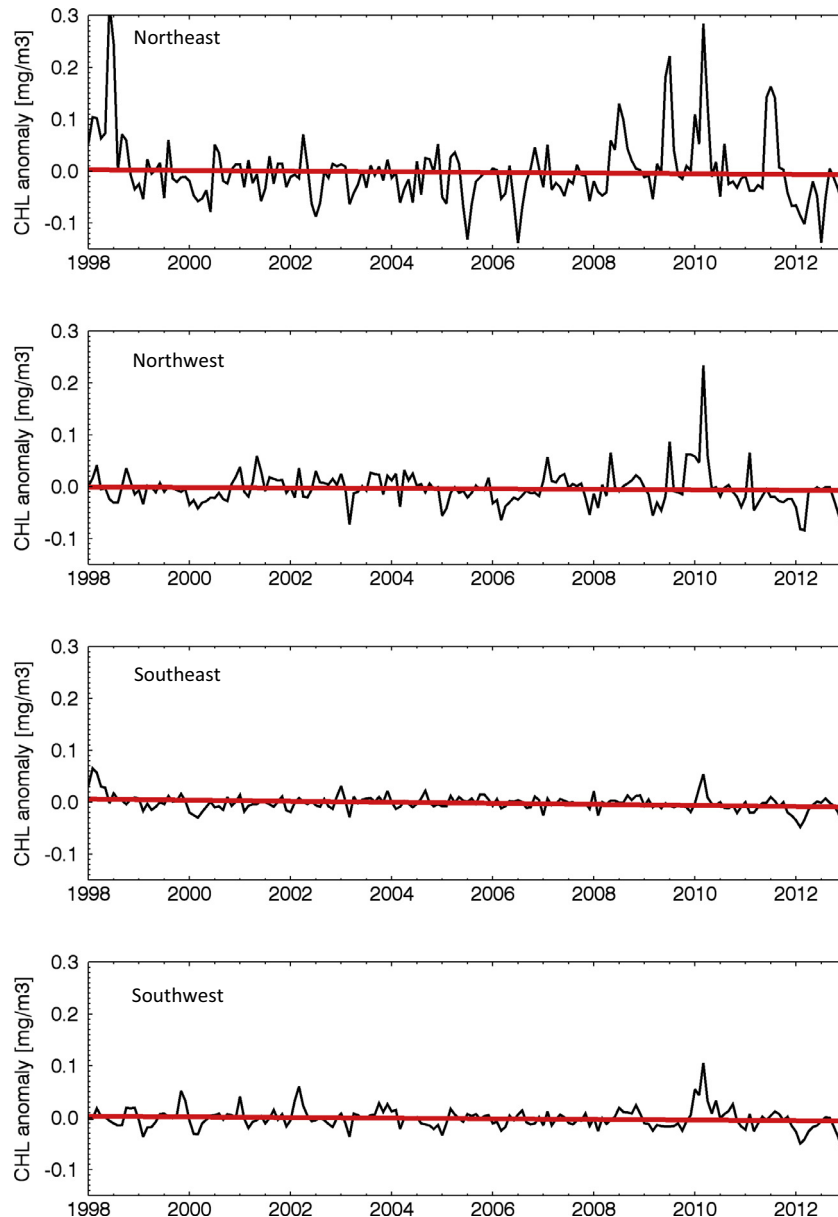


Fig. 12. Chlorophyll-*a* concentration anomaly [mg m^{-3}] series derived from SeaWiFS (1998–2002) and MODIS (2003–2013) data. The least squares regression (January 1998–January 2013) lines for the respective ROIs are overlaid. None of the slopes were significantly different from zero.

in chlorophyll-*a* concentration in all areas. In the northeastern quadrant, a substantial mid-summer secondary peak in NPP of $\sim 500 \text{ mg C m}^{-2} \text{ d}^{-1}$ was observed simultaneous with the July chlorophyll-*a* peak. This may be an artifact in the NPP values related to the regular offshore transport of coastal and riverine waters observed in July and August over the CZCS, SeaWiFS, and MODIS time series, but, regardless, this is a highly productive region of the Gulf in terms of fisheries.

As with chlorophyll concentration, there is no evidence of any long-term change in NPP values with time in any of the quadrants (Fig. 13). Since our regions of interest trace the 1000 m isobaths, variability in chlorophyll-*a* concentration in the southeastern and southwestern quadrants reflects only blooms caused by deep ocean mixing or extreme cross-shelf transport events. In the southeastern quadrant, the time series of chlorophyll concentration shows only small anomalies relative to the monthly climatology (Fig. 12). This region experiences events north of the Yucatan

Peninsula (north of 24.5°N). For example, the positive anomaly of January–March 2010 is the result of convective mixing due to cold SST (SST anomalies of -1°C) and strong winds observed Gulf-wide at the end of 2009 and through January 2010 (see below). Some of the positive anomalies in the southeastern region of the Gulf are due to the high chlorophyll concentrations associated with the upwelling phenomenon that begins along the western edge of the Yucatan Current and propagates offshore along the periphery of the Loop Current (Perez et al.; 1999a,b). This upwelling extends along the cyclonic edge of the Loop Current beyond the Yucatan shelf break. The bloom traces a sinuous arc that can extend over 1800 km into the northwestern and northeastern Gulf. SeaWiFS and MODIS data show that this long bloom occurs most often during January–March periods. This pattern was also clearly visible in the CZCS data. This bloom is advected and then likely sustained by upwelling along the cyclonic edge of the Loop Current. Many satellite images showed this bloom merging with the colored plume of

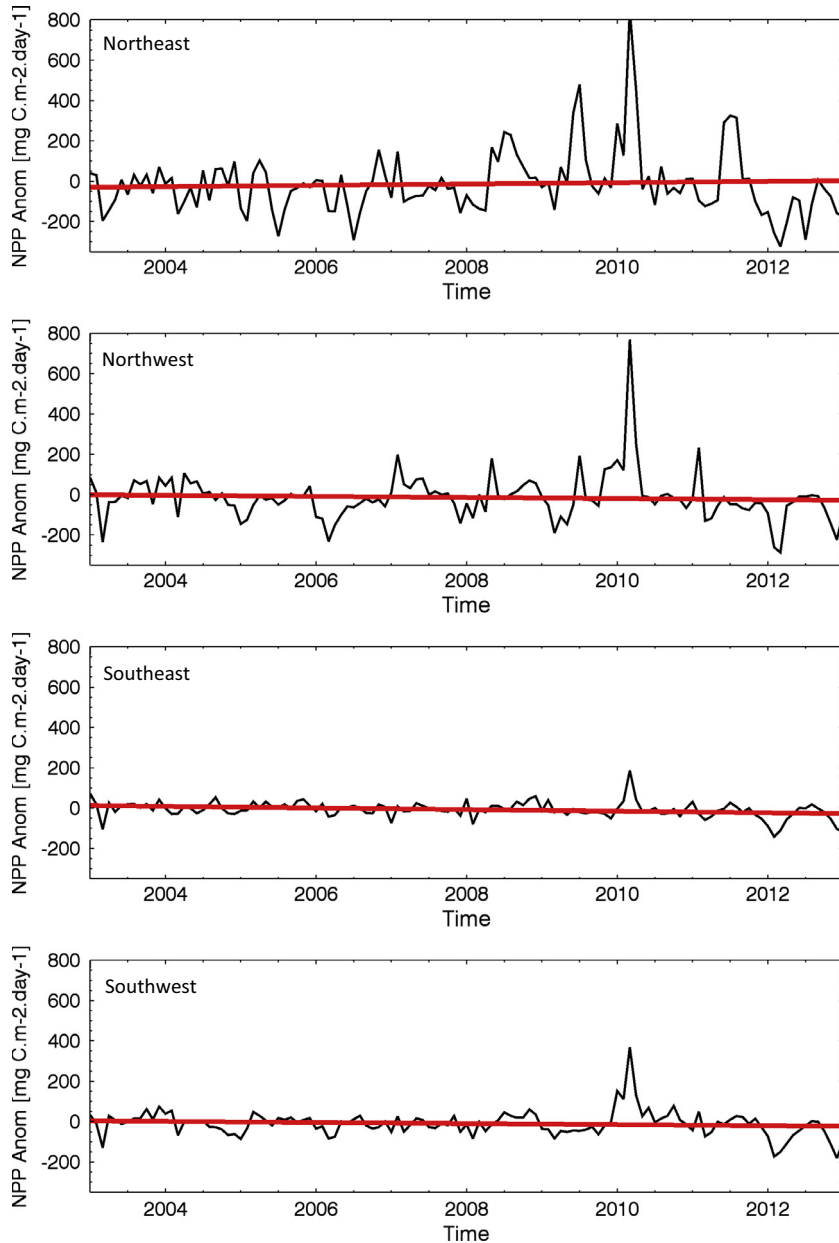


Fig. 13. Net Primary Production anomaly [$\text{mg C m}^{-2} \text{d}^{-1}$] series derived from MODIS observations (2003–2013; black line) data. The least squares regression (January 2002–January 2013) lines for the respective ROIs are overlaid. None of the slopes were significantly different from zero.

water advected offshore from the Mississippi River delta region as this plume became entrained along the northern edge of the Loop Current, typically in the July timeframe.

At the end of 2009 and beginning of 2010, the entire Gulf of Mexico experienced the largest positive chlorophyll-*a* anomalies seen since the SeaWiFS record started in 1998 (Fig. 12). This large positive anomaly was synchronous throughout the Gulf. A much smaller basin-wide positive anomaly was also observed in 1998–1999. The 2010 anomaly started as early as November–December of 2009 and was most pronounced between January and March 2010. During the intervening months, the Gulf of Mexico experienced the coolest SST anomalies observed in the near three-decade-long SST record (i.e. -1 to -2 °C relative to the climatology for these months; Fig. 9). This coincided with stronger than average basin-wide winds (sustained 0 to $+1 \text{ m s}^{-1}$; Fig. 8). Another basin-wide cool anomaly, although somewhat less pronounced than the one of 2010, was observed during January–February of 2011

(between -1 and -1.5 °C relative to the climatology; Fig. 9). This period experienced lower than average winds throughout the Gulf (0 to $<-1 \text{ m s}^{-1}$; Fig. 8). The conditions in 2011 likely led to shallower winter mixing relative to 2009–2010. The winter bloom of 2010–2011 was also less pronounced relative to the one seen in 2009–2010. These observations are consistent with the observation that increased mixing of the upper water column due to storms leads to higher chlorophyll-*a* concentrations in the deep Gulf of Mexico (Melo Gonzalez et al., 2000).

The 10-year MODIS NPP time series showed marked differences between the quadrants of the Gulf of Mexico, but it also showed some periods during which changes occurred simultaneously throughout the Gulf. All regions show a marked peak in the January–March 2010 interval, with average NPP exceeding $1400 \text{ mg C m}^{-2} \text{ d}^{-1}$ over the entire northern Gulf of Mexico in February that year (Fig. 13). Coherent minima (an anomaly of $-200 \text{ mg C m}^{-2} \text{ d}^{-1}$) occurred in all quadrants of the Gulf in

February–March of 2003, March 2006, and January–February 2012. This last minimum was the most pronounced of the series. The frequent anomalies in January–February are driven in part by the effect of the very large Gulf-wide peak observed in 2010 on the monthly climatologies. The pronounced NPP minimum of January–February 2012 occurred when SST in the Gulf of Mexico were high relative to the norm (+1 °C anomalies) and winds in the Gulf of Mexico were very weak (<6.5 m s⁻¹ according to NOAA NDBC Buoy 42001 located in the Central Gulf; not shown). In contrast, average NPP values were observed in each region for January–February 2011, a period that experienced equally weak winds but instead large SST negative anomalies (i.e. colder than -1 °C; Figs. 8 and 9).

Climate indices

We found no significant correlation at the monthly scale between any of the parameters we examined in the Gulf of Mexico and either the monthly MEI or the monthly AMO indices, including at lags spanning 0 to ±8 months. However, the AMO shows a positive long-term trend over the period of the satellite record examined (1981–2012). While all quarters of the Gulf of Mexico showed positive trends in SST anomalies similar to that of the AMO (Fig. 9), only the southeastern quadrant showed a trend that was not significantly different to that of the AMO at the 95% level. While there is no direct correlation between the monthly MEI and the SST anomalies in the Gulf, the trend in the MEI over our study period between 1981 and 2012 was strongly negative (not shown).

Discussion

Long-term changes in seasonal meteorological patterns, in the average temperature of surface waters, or in the standing stock and productivity of phytoplankton have important impacts on the habitat for numerous species, including humans. Long-term change can affect reproductive success, feeding habits, species interactions, migration routes, and ultimately define whether an organism may be present in a region at all or not. Studies such as that of Gable (1993) provide the earliest chart of the major ecological domains in the Gulf of Mexico, but these charts need to be redrafted frequently to help understand where change is taking place. Long-term observations and baselines help develop the dynamic biogeographical regions needed to assess effects of disturbance due to natural events or anthropogenic causes including resource development (Muller-Karger et al., 2014).

The waters of the interior of the Gulf of Mexico seaward of the continental margin continue to be seriously undersampled. A search for observations of chlorophyll concentration in the NOAA NODC archives shows fewer than 100 chlorophyll observations for each of the Regions of Interest defined for this study (Fig. 1). Most of these samples are associated with a particular cruise or with a seasonal program, such as the NOAA SEAMAP (SouthEast Area Monitoring and Assessment Program). We were not able to derive a good chlorophyll concentration dataset from historical field observations archived at the NOAA NODC to compare with either CZCS, SeaWiFS, or MODIS chlorophyll estimates. Most samples in the Gulf of Mexico available at the NODC are from the northern and eastern shelf regions, with relatively few samples available from offshore waters. Thus, information derived from remote sensing is essential for characterization of the deep water areas of the Gulf.

There was no significant trend in the chlorophyll-a concentration time series for any of the regions in the Gulf of Mexico, either during the CZCS years (1978–1986), or during the SeaWiFS and MODIS years (1998–2012 inclusive). We also found no apparent trend in the NPP record. The lack of long term trends in chlorophyll

and NPP is in contrast to trends in physical variables that are important to biological processes. Particularly, over the past 20 years we have seen an increase in sea surface temperature of +0.6 °C, in the sea surface height anomaly of +0.06 m, and in winter-time wind speed of up to +0.7 m s⁻¹. The SeaWiFS observations are calibrated, stable, and sufficiently accurate to conduct long-term, climate record analyses (Hu et al., 2001; Franz et al., 2007; Eplee et al., 2011; Siegel et al., 2013). The MODIS calibration was cross-referenced to that of SeaWiFS. The chlorophyll-a and NPP products used in this analysis were generated by the latest NASA reprocessing of these ocean color data (MODIS 2013 reprocessing). Therefore, these results imply that, on average, annual phytoplankton concentration and productivity are insensitive to the long-term changes in physical variables such as wind speed and SST observed over this period in the Gulf of Mexico. Below we explore a possible reason for the lack of change observed over the past 15 years in average phytoplankton pigment concentration and Net Primary Production in the offshore Gulf of Mexico.

The time series of chlorophyll values show very regular seasonal changes in the southern quarters of the Gulf. Years with extremely cold winters, like the winter of 2009–2010, showed a positive anomaly in all areas. The cold temperatures observed in 2011 only seem to have led to markedly higher chlorophyll concentrations only in the northern quadrants. We observed winds during the 2009–2010 winter that were anomalously high in all quadrants. Winds during winter of 2010–2011 were much milder, and showed a smaller to nil anomaly. In general, we observed higher chlorophyll concentrations and primary productivity only during periods when cooler temperature and higher winds coincided. We saw normal levels of chlorophyll when winds were average. And we measured low chlorophyll concentration when temperatures were warm and winds were weak at the same time.

Melo Gonzalez et al., 2000 had already found positive anomalies in pigment concentration in the Gulf of Mexico during winter months. This was associated with intense mixing of the water column by higher frequency and stronger winds associated with cold fronts. They found a 4–5 month lag between low SST, high chlorophyll concentrations, and the ENSO warm phase of 1982–1983 (Enfield and Mayer, 1997) for the Caribbean and Gulf of Mexico. Another positive pigment anomaly was observed in 1980–1981. This anomaly was not related to ENSO, but rather to a period of higher hurricane and extra-tropical low-pressure activity. Using a longer time series, we could not find a generalized relationship between any of our parameters and the monthly ENSO MEI or AMO indices in the Gulf of Mexico at lags spanning 0 to +8 months. The positive trend in the AMO during the period overlapping the Pathfinder SST data (1981–2012) is consistent with the AMO warm phase that started in the mid-90s (Enfield and Cid-Serrano, 2010). Over such time scales, the Gulf of Mexico reflects changes in heat balance taking place over the North Atlantic. The link between the North Atlantic and the Gulf of Mexico occurs through variations in the advective throughflow between the Yucatan Channel and the Straits of Florida (Liu et al., 2012). Because that flow is part of the Atlantic Ocean meridional overturning circulation, the AMO acts over timescales longer than a year. The negative trend in the MEI over our study period is due to the repeated strong warm El Niño–Southern Oscillation (ENSO) events observed in the 1980s and 1990s, and higher frequency of cooler ENSO events since 1999–2000, including the strong negative events of 1999–2000, 2007–2008, 2010–2011, and 2011–2012. Such extraneous factors (e.g., ENSO extremes) affect the annual heat budget of the Gulf of Mexico going into summer (Melo Gonzalez et al., 2000). They cause sporadic responses that have little or nothing to do with the North Atlantic. Air-sea interactions driving changes in the Gulf of Mexico at any particular time differ from those acting on average over the

North Atlantic. Whether the changes inferred from these two climate indices are related is not yet clear.

In any event, the results from [Muller-Karger et al. \(1991\)](#) and [Melo Gonzalez et al., 2000](#) pointed to the depth of the mixed layer as a controlling factor in defining chlorophyll-*a* levels in the Gulf of Mexico. In this study we found the relationship between the MLD estimates derived from the ECCO2 model and Chl-*a* concentration, and MLD and NPP, to be strong in every quadrant of the Gulf of Mexico. Some outliers in this relationship stood out only in the northeastern quadrant. These results were consistent with the Sverdrup critical depth hypothesis ([Sverdrup, 1953](#)). There is sufficient light on a year-round basis to illuminate the mixed layer in the Gulf of Mexico. Thus the ‘spring bloom’ occurs in the middle of winter, when the mixed layer is deepest, allowing for a greater influx of nutrients into the euphotic zone, as [Muller-Karger et al. \(1991\)](#) had already described.

The statistical relationship between NPP and MLD is slightly stronger than that of chlorophyll-*a* concentration. [Table 1](#) shows the coefficients derived from a linear regression analysis performed between NPP and MLD ([Fig. 14](#)). We chose to cast NPP as the independent variable and MLD as the dependent variable because ocean color NPP observations are readily available, while MLD estimates are difficult to obtain, particularly in a synoptic manner. We found that except in the northeast, NPP can predict MLD well, explaining upwards of 70% of the variability in the MLD derived in the ECCO2 model. The relationship is less robust in the northeastern quadrant, where high levels of chlorophyll-*a* and NPP occurred regularly in July and August, during periods of shallow MLD ([Fig. 14](#)). Visual examination of the satellite data time series confirms that the high positive chlorophyll-*a* and NPP anomalies observed in summer 1998, 2008, 2009, and 2011 in this region were related to east and southward dispersal of Mississippi water.

[Muller-Karger et al. \(1991\)](#), [Biggs et al. \(1993\)](#), [Muller-Karger \(2000\)](#), [Del Castillo et al. \(2001\)](#), [Salisbury et al. \(2004\)](#), [Hu et al. \(2005\)](#), [D'Sa and Korobkin \(2009\)](#), and [Martínez-López and](#)

[Zavala-Hidalgo \(2009\)](#) describe the temporal variability in apparent chlorophyll-*a* concentration in coastal and shelf waters around the Gulf of Mexico and the mechanisms by which coastal waters are advected across the shelf. The chlorophyll-*a* concentration climatology ([Fig. 6](#)) and the time series of anomalies ([Fig. 12](#)) clearly show that the largest deviations from the mean and the highest temporal variability is observed in the northeastern quadrant of the Gulf of Mexico. [Muller-Karger et al. \(1991\)](#), [Muller-Karger \(2000\)](#), [Del Castillo et al. \(2001\)](#), and [Hu et al. \(2005\)](#) had observed the offshore entrainment of Mississippi plume water into the interior of the Gulf and subsequent advection to the southeast in the Loop Current. We observed this entrainment in 11 out of the 14-years of the series of SeaWiFS and MODIS images (1998–2012 inclusive). It is this feature that leads to a different climatological chlorophyll pattern than expected for clear offshore waters, and the cause for which [Salmerón-García et al. \(2011\)](#) and [Callejas-Jimenez et al. \(2012\)](#) identified the northeastern Gulf of Mexico as a uniquely different deep-water region in the Gulf.

Cross-shelf advection of coastal waters is forced by the seasonal convergence of alongshore winds particularly to the southwest of the Mississippi Delta, off the US-Mexico border region, and in the Bay of Campeche ([D'Sa and Korobkin, 2009](#); [Martínez-López and Zavala-Hidalgo; 2009](#)). In the northeastern Gulf of Mexico, offshore advection of waters from the Mississippi River and other coastal waters is related to offshore transport due primarily to local wind. These waters can subsequently be entrained in the Loop Current or its eddies ([Muller-Karger, 2000](#)), or in the southward drifts that occur over the west Florida shelf ([Gilbes et al., 1996](#)).

One question left unresolved by the observations reported here is whether the effect of increasing stability of the upper water column due to rising surface temperatures is offset by the increase in the anticyclonic mesoscale activity in the interior of the Gulf or by the gradual increase in winds. The trend toward a warmer and more windy Gulf of Mexico is not reflected in the biological indicators Chl-*a* and NPP. We do not yet have a conceptual model that can provide an explanation for which process may dominate. This

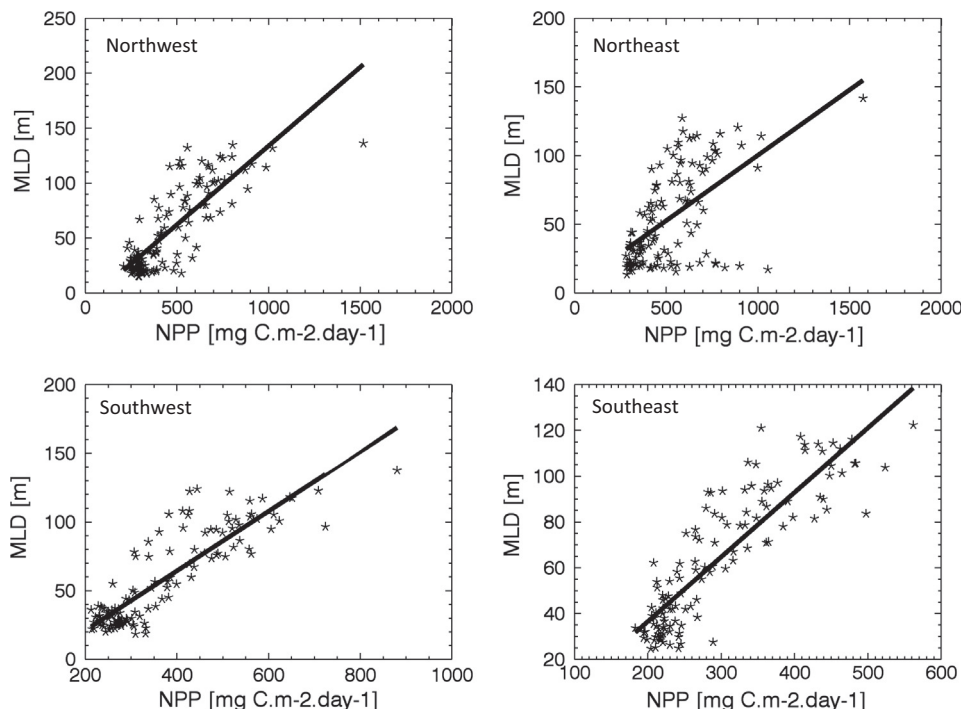


Fig. 14. Monthly mean MODIS-derived Net Primary Production (NPP, [$\text{mg C m}^{-2} \text{ day}^{-1}$]) against monthly mean ECCO2 mixed layer depth (MLD, [m]) in each of the Gulf of Mexico quarters. Parameters for the least-squares linear regression are shown in [Table 1](#).

question is relevant for assessing impacts of climate change over both regional and global scales.

The increase in oceanic sea surface temperature has already been highlighted as a driver of a possible increase in hurricane activity (Goldenberg et al., 2001). More generally, the trend toward stronger winds over large areas of the ocean (Young et al., 2011a,b) and higher upper ocean temperatures (Levitus et al., 2001; Roemmich et al., 2012) are linked through intensification of the Walker and Hadley cells in the atmosphere (England et al., 2014). England et al. (2014) attribute cooling of surface waters in the equatorial Pacific to the intensification of the Trade Winds observed in the Pacific in the 2001–2012 timeframe.

The significant warming and increase in the sea surface height anomaly that we observe in the interior of the Gulf also helps to explain the rising coastal sea levels observed by Hanson and Maul (1993), Maul et al. (2001), and Wahl et al. (2014). Part of the increase in the sea surface height anomaly is a direct consequence of steric changes due to this warming of the water column. Sea level rise due to climate change is one of the most important threats to ecosystem services provided at present by coastal areas of the Gulf of Mexico (Twilley et al., 2001). Yet, how this affects basic processes like primary production in the interior of the Gulf of Mexico is not clear. We know that changes in mesoscale eddy variability play an important role in providing nutrients for phytoplankton growth (McGillicuddy et al., 1999; Mahadevan et al., 2012, 2010). Piontovski and Nezlin (2012) found a positive correlation between negative SSHA and chlorophyll concentration in the western Arabian Sea, emphasizing that chlorophyll was generally lower in years where SSHA was more positive (i.e. anticyclonic eddies dominate) than negative (i.e. cyclonic eddies dominate). In the Canary Eddy Corridor, chlorophyll concentration may be enhanced by both anticyclonic and cyclonic eddies (Sangrà et al., 2009). Examining the hypothesis that anticyclonic or cyclonic eddies, or both, have an impact on chlorophyll requires a synoptic eddy census in the Gulf of Mexico, which was outside the scope of the present study. Again, these questions are relevant to global change science because these processes apply to regional seas generally and the impacts of concurrent change are important at basin and global spatial scales.

The results that there has been no change over the past 20 years in average mixed layer depth is thus very consistent with the observation that there have been no long-term trends in chlorophyll concentration or in the overall phytoplankton productivity of offshore waters of the Gulf. However, answering the question of whether the increase in the wind stress can offset the decrease in regional primary productivity that would be expected solely from increased thermal stability of surface waters probably requires a detailed study using a dynamic mixed layer model. We encourage such a study as this is at the core of the future health of the Gulf of Mexico ecosystem.

Acknowledgements

This work was supported by ExxonMobil Upstream Research Company, NASA grant NNX14AP62A ‘National Marine Sanctuaries as Sentinel Sites for a Demonstration Marine Biodiversity Observation Network (MBON)’ funded under the National Ocean Partnership Program (NOPP RFP NOAA-NOS-IOOS-2014-2003803 in partnership between NOAA, BOEM, and NASA), NASA grant NNX11AP76G ‘Management and conservation of Atlantic Bluefin tuna (*Thunnus thynnus*) and other highly migratory fish in the Gulf of Mexico under IPCC climate change scenarios’, and NOAA (AOML/CIMAS Grant ‘Ocean Conditions in The Gulf of Mexico’). Ocean circulation simulation results were kindly provided by the *Estimating the Circulation and Climate of the Ocean, Phase II (ECCO2)* Project.

References

- Adams, C.M., Hernandez, E., Cato, J.C., 2004. The economic significance of the Gulf of Mexico related to population, income, employment, minerals, fisheries and shipping. *Ocean and Coastal Management* 47 (11–12), 565–580. <http://dx.doi.org/10.1016/j.ocecoaman.2004.12.002>.
- Alvera-Azcárate, A., Barth, A., Weisberg, R.H., 2009. The surface circulation of the Caribbean Sea and the Gulf of Mexico as inferred from satellite altimetry. *Journal of Physical Oceanography* 39 (3), 640–657.
- Atlas, R., Hoffman, R.N., Ardizzone, J., Leidner, S.M., Jusem, J.C., Smith, D.K., Gombos, D., 2011. A cross-calibrated, multiplatform ocean surface wind velocity product for meteorological and oceanographic applications. *Bulletin of the American Meteorological Society* 92, 157–174. <http://dx.doi.org/10.1175/2010BAMS2946.1>.
- Baringer, M.O.N., Larsen, J.C., 2001. Sixteen years of Florida current transport at 27°N. *Geophysical Research Letters* 28 (16), 3179–3182. <http://dx.doi.org/10.1029/2001GL013246>.
- Behrenfeld, M.J., Falkowski, P.G., 1997. Photosynthetic rates derived from satellite-based chlorophyll concentration. *Limnology and Oceanography* 42, 1–20.
- Behringer, D.W., Molinari, R.L., Festa, J.F., 1977. The variability of anticyclonic current patterns in the Gulf of Mexico. *Journal of Geophysical Research* 82, 5469–5476.
- Biggs, D.C., Muller-Karger, F.E., 1993. Ship and satellite observations of chlorophyll stocks in warm- and cold-core rings in the western Gulf of Mexico. *Journal of Geophysical Research* 99 (C4), 7371–7384.
- Biggs, D.C., Jochens, A.E., Howard, M.K., DiMarco, S.F., Mullin, K.D., Leben, R.R., Muller-Karger, F.E., Hu, C., 2005. Eddy forced variations in on- and off-margin summertime circulation along the 1000-m Isobath of the Northern Gulf of Mexico, 2000–2003, and links with sperm whale distributions along the middle shelf. In: Sturges, W., Lugo-Fernandez, A. (Eds.), *New Developments in the Circulation of the Gulf of Mexico*. AGU Geophysical Monograph Series 161, pp. 71–86.
- Bunge, L., Ochoa, J., Badan, A., Candela, J., Sheinbaum, J., 2002. Deep flows in the Yucatan Channel and their relation to changes in the loop current extension. *Journal of Geophysical Research* 107.
- Callejas-Jimenez, M., Santamaría-del-Ángel, E., González-Silvera, A., Millán-Núñez, R., Cajal-Medrano, R., 2012. Dynamic regionalization of the Gulf of Mexico based on normalized radiances (nLw) derived from MODIS-Aqua. *Continental Shelf Research* 37, 8–14. <http://dx.doi.org/10.1016/j.csr.2012.01.014>.
- Candela, J., Tanahara, S., Crepon, M., Barnier, B., Sheinbaum, J., et al., 2003. Yucatan Channel flow: observations versus CLIPPER ATL6 and MERCATOR PAM models. *Journal of Geophysical Research* 108 (C12), 24pp. <http://dx.doi.org/10.1029/2003JC001961>.
- Cardona, Y., Bracco, A., 2014. Predictability of mesoscale circulation throughout the water column in the Gulf of Mexico. *Deep Sea Research Part II: Topical Studies in Oceanography*. <http://dx.doi.org/10.1016/j.dsrr.2014.01.008>.
- Casey, K.S., Brandon, T.B., Cornillon, P., Evans, R., 2010. The past, present and future of the AVHRR Pathfinder SST program. In: Barale, V., Gower, J.F.R., Alberotanza, L. (Eds.), *Oceanography From SPACE*. Springer. http://dx.doi.org/10.1007/978-90-481-8681-5_16.
- Cerdeira-Estrada, S., Muller-Karger, F.E., Gallegos Garcia, A., 2005. Variability of the sea surface temperature around cuba. *Gulf of Mexico Science* 23 (2), 161–171.
- Chang, Y.-L., Oey, L.-Y., 2010. Eddy and wind-forced heat transports in the Gulf of Mexico. *Journal of Physical Oceanography* 40, 2728–2742. <http://dx.doi.org/10.1175/2010JPO4474.1>.
- Chang, Y.L., Oey, L.Y., 2012. Why does the Loop Current tend to shed more eddies in summer and winter? *Geophysical Research Letters* 39 (5).
- Chang, Y.L., Oey, L.Y., 2013a. Loop Current growth and eddy shedding using models and observations: numerical process experiments and satellite altimetry data. *Journal of Physical Oceanography* 43 (3), 669–689.
- Chang, Y.L., Oey, L.Y., 2013b. Coupled response of the trade wind, SST Gradient, and SST in the Caribbean Sea, and the potential impact on Loop Current's interannual variability. *Journal of Physical Oceanography* 43 (7), 1325–1344.
- Chérubin, L.M., Sturges, W., Chassignet, E.P., 2005. Deep flow variability in the vicinity of the Yucatan Straits from a high-resolution numerical simulation. *Journal of Geophysical Research – Part C-Oceans* 110, C04009.
- Chollett, I., Müller-Karger, F.E., Heron, S.F., Skirving, W., Mumby, P.J., 2012. Seasonal and spatial heterogeneity of recent sea surface temperature trends in the Caribbean Sea and southeast Gulf of Mexico. *Marine Pollution Bulletin*. <http://dx.doi.org/10.1016/j.marpolbul.2012.02.016>.
- Cloern, J.E., Grenz, C., Vidergar-Lucas, L., 1995. An empirical model of the phytoplankton chlorophyll:carbon ratio—the conversion factor between productivity and growth rate. *Limnology and Oceanography* 40 (7), 1313–1321.
- Conkright, M.E., Locarnini, R.A., Garcia, H.E., O’Brien, T.D., Boyer, T.P., Stephens, C., Antonov, J.I., 2002. World Ocean Atlas 2001: Objective Analyses, Data Statistics, and Figures, CD-ROM Documentation. National Oceanographic Data Center, Silver Spring, MD, 17 pp.
- Del Castillo, C., Gilbes, F., Coble, P., Muller-Karger, F.E., 2000. On the dispersal of riverine colored dissolved organic matter over the West Florida Shelf. *Limnology and Oceanography* 45 (6), 1425–1432.
- Del Castillo, C., Coble, P., Conney, R., Muller-Karger, F.E., Vanderbloemen, L., Vargo, G., 2001. Multispectral in-situ measurements of organic matter and chlorophyll fluorescence in seawater: documenting the intrusion of the Mississippi River Plume in the West Florida Shelf. *Limnology and Oceanography* 46 (7), 1836–1843.

- Ding, K., Gordon, H.R., 1995. Analysis of the influence of O₂ A-band absorption on atmospheric correction of ocean-color imagery. *Applied Optics* 34, 2068–2080.
- D'Sa, E.J., Korobkin, M., 2009. Examining SeaWiFS chlorophyll variability along the Louisiana coast using wavelet analysis. In: Proceedings, OCEANS 2009, MTS/IEEE Biloxi – Marine Technology for Our Future: Global and Local Challenges, 1–5.
- Enfield, D.B., Cid-Serrano, L., 2006. Projecting the risk of future climate shifts. *International Journal of Climatology* 26 (7), 885–895.
- Enfield, D.B., Cid-Serrano, L., 2010. Secular and multidecadal warmings in the North Atlantic and their relationships with major hurricane activity. *International Journal of Climatology* 30, 174–184.
- Enfield, D.B., Mayer, D.A., 1997. Tropical Atlantic SST variability and its relation to El Niño-Southern oscillation. *Journal of Geophysical Research* 102, 929–945.
- Enfield, D.B., Mestas-Nunez, A.M., Trimble, P.J., 2001. The Atlantic multidecadal oscillation and its relationship to rainfall and river flows in the continental U.S. *Geophysical Research Letters* 28, 2077–2080.
- England, M.H., McGregor, S., Spence, P., Meehl, G.A., Timmermann, A., Cai, W., Sen Gupta, A., McPhaden, M.J., Purich, A., Santoso, A., 2014. Recent intensification of wind-driven circulation in the Pacific and the ongoing warming hiatus. *Nature Climate Change* 4. <http://dx.doi.org/10.1038/NCLIMATE2106>.
- Eplee, R.E., Jr., Meister, G., Patt, F.S., Franz, B.A., McClain, C.R., 2011. Uncertainty assessment of the SeaWiFS on-orbit calibration. In: Butler, J.J., Xiong, X., Gu, X. (Eds.), *Earth Observing Systems XVI*. Proc. SPIE, 8153. pp. 815310.
- Etter, P.C., 1983. Heat and freshwater budgets of the Gulf of Mexico. *Journal of Physical Oceanography* 13, 2058–2069.
- Ezer, T., 2000. On the seasonal mixed-layer simulated by a basin-scale ocean model and the Mellor-Yamada turbulence scheme. *Journal of Geophysical Research* 105 (C7), 16843–16855.
- Ezer, T., Oey, L.-Y., Lee, H.-C., Sturges, W., 2003. The variability of currents in the Yucatan Channel: analysis of results from a numerical Ocean model. *Journal of Geophysical Research* 108 (C1), 3012. <http://dx.doi.org/10.1029/2002JC001509>.
- Falkowski, P.G., Dubinsky, Z., Wyman, K., 1985. Growth-irradiance relationships in phytoplankton. *Limnology and Oceanography* 30, 311–321.
- Felder, D.L., Camp, D.K. (Eds.), 2012. *Gulf of Mexico Origin, Waters, and Biota Biodiversity*. Texas A&M University Press.
- Franz, B.A., Bailey, S.W., Werde, P.J., McClain, C.R., 2007. Sensor-independent approach to vicarious calibration of satellite ocean color radiometry. *Applied Optics* 46, 5068–5082.
- Fratantonio, P.S., Lee, T.N., Podesta, G.P., Muller-Karger, F., 1998. The influence of Loop Current variability on the formation and evolution of cyclonic eddies in the Southern Straits of Florida. *Journal of Geophysical Research* 103 (C11), 24759–24779.
- Gable, F.J., 1993. Marine habitats: selected environmental and ecological charts. In: Maul, George (Ed.), *Climate Change in the Intra-Americas Sea*. United Nations Environmental Programme (Wider Caribbean Region) and Intergovernmental Oceanographic Commissions (Caribbean and Adjacent Regions). Edward Arnold Publishers, pp. 217–261 (Chapter 10).
- Gilbes, F., Tomas, C., Walsh, J.J., Muller-Karger, F.E., 1996. An episodic chlorophyll plume on the west Florida shelf. *Continental Shelf Research* 16 (9), 1201–1224.
- Goldenberg, S.B., Landsea, C.W., Mestas-Nunez, A.M., Gray, W.M., 2001. The recent increase in Atlantic hurricane activity: causes and implications. *Science* 293, 474–479.
- Gordon, H.R., 1997. Atmospheric correction of ocean color imagery in the earth observing system era. *Journal of Geophysical Research* 102, 17081–17106.
- Gordon, H.R., Wang, M., 1994. Retrieval of water-leaving radiance and aerosol optical thickness over the oceans with SeaWiFS: a preliminary algorithm. *Applied Optics* 33, 443–452.
- Gordon, H.R., Brown, O.B., Evans, R.H., Brown, J.W., Smith, R.C., Baker, K.S., Clark, D.K., 1988. A semianalytic radiance model of ocean color. *Journal of Geophysical Research* 93 (D9), 10909–10924.
- Gregg, W.W., Conkright, M.E., 2001. Global seasonal climatologies of ocean chlorophyll: blending in situ and satellite data for the CZCS era. *Journal of Geophysical Research* 106, 2499–2515.
- Gregg, W.W., Conkright, Margarita E., O'Reilly, John E., Patt, Frederick S., Wang, Menghua H., Yoder, James A., Casey, Nancy W., 2002. NOAA–NASA coastal zone color scanner reanalysis effort. *Applied Optics* 41 (9), 1615–1628.
- Hanson, K., Maul, G.A., 1993. Analysis of temperature, precipitation, and sea level variability with concentration on Key West, Florida, for evidence of trace-gas-induced climate change. In: Maul, George (Ed.), *Climate Change in the Intra-Americas Sea*. United Nations Environmental Programme (Wider Caribbean Region) and Intergovernmental Oceanographic Commissions (Caribbean and Adjacent Regions). Edward Arnold Publishers, pp. 193–213 (Chapter 9).
- Herring, J.H., 2010. Gulf of Mexico hydrographic climatology and method of synthesizing subsurface profiles from the satellite sea surface height anomaly. US. Department of Commerce. National Oceanic and Atmospheric Administration. National Ocean Service. Coastal Survey Development Laboratory. Report 122, 63 pp.
- Hu, C., Carder, K.L., Muller-Karger, F.E., 2001. How precise are SeaWiFS ocean color estimates? Implications of digitization-noise errors. *Remote Sensing of Environment* 76, 239–249.
- Hu, C., Nelson, J.R., Johns, E., Chen, Z., Weisberg, R.H., Muller-Karger, F.E., 2005. Mississippi River water in the Florida Straits and in the Gulf Stream off Georgia in summer 2004. *Geophysical Research Letters* 32 (10), L14606. <http://dx.doi.org/10.1029/2005GL022942>.
- Hu, C., Muller-Karger, F., Murch, B., Myhre, D., Taylor, J., Luerssen, R., Moses, C., Zhang, C., Gramer, L., Hendee, J., 2009. Building an automated integrated observing system to detect sea surface temperature anomaly events in the Florida keys. *IEEE Transactions on Geoscience and Remote Sensing* 47 (6), 1607–1620, June 2009.
- Hurlburt, H.E., Thompson, J.D., 1980. A numerical study of loop current intrusions and eddy shedding. *Journal of Physical Oceanography* 10, 1611–1651.
- Kalnay, E., Kanamitsu, M., Kistler, R., Collins, W., Deaven, D., Gandin, L., Iredell, M., Saha, S., White, G., Woollen, J., Zhu, Y., Chelliah, M., Ebisuzaki, W., Higgins, W., Janowiak, J., Mo, K.C., Ropelewski, C., Wang, J., Leetmaa, A., Reynolds, R., Jenne, R., Joseph, Dennis, 1996. The NCEP/NCAR 40-year reanalysis project. *Bulletin of the American Meteorological Society* 77 (3), 437–471.
- Kara, A.B., Rochford, P.A., Hurlburt, H.E., 2000. An optimal definition for ocean mixed layer depth. *Journal of Geophysical Research* 105 (C7), 16803–16821. <http://dx.doi.org/10.1029/2000JC900072>.
- Karnauskas, M., Schirripa, M.J., Kelble, C.R., Cook, G.S., Craig, J.K., 2013. Ecosystem status report for the Gulf of Mexico. NOAA Technical Memorandum NMFS-SEFSC-653.
- Kennedy, A.J., Griffin, M.L., Morey, S.L., Smith, S.R., O'Brien, J.J., 2007. Effects of El Niño-southern oscillation on sea level anomalies along the Gulf of Mexico coast. *Journal of Geophysical Research: Oceans* 112 (C5), 112. <http://dx.doi.org/10.1029/2006JC003904>.
- Kistler, R., Collins, W., Saha, S., White, G., Woollen, J., Kalnay, E., Chelliah, M., Ebisuzaki, W., Kanamitsu, M., Kousky, V., van den Dool, H., Jenne, R., Fiorino, M., 2001. The NCEP-NCAR 50-year reanalysis: monthly means CD-ROM and documentation. *Bulletin of the American Meteorological Society* 82 (2), 247–267 (February 2001).
- Laws, E.A., Bannister, T.T., 1980. Nutrient- and light-limited growth of *Thalassiosira fluviatilis* in continuous culture, with implications for phytoplankton growth in the ocean. *Limnol and Oceanography* 25, 457–473.
- Levitus, S., Antonov, J.I., Wang, J., Delworth, T.L., Dixon, K.W., Broccoli, A.J., 2001. Anthropogenic warming of Earth's climate system. *Science* 292, 267–270.
- Levitus, S., Antonov, J.I., Boyer, T.P., Locarnini, R.A., Garcia, H.E., Mishonov, A.V., 2009. Global ocean heat content 1955–2008 in light of recently revealed instrumentation problems. *Geophysical Research Letters* 36, L07608. <http://dx.doi.org/10.1029/2008GL037155>.
- Le Hénaff, M., Kourafalou, V.H., Morel, Y., Srinivasan, A., 2012. Simulating the dynamics and intensification of cyclonic Loop Current Frontal Eddies in the Gulf of Mexico. *Journal of Geophysical Research: Oceans* (1978–2012) 117 (C2).
- Le Traon, P.Y., Nadal, F., Ducet, N., 1998. An improved mapping method of multi-satellite altimeter data. *Journal of Atmospheric and Oceanic Technology* 15, 522–534.
- Li, Q.P., Franks, P.J.S., Landry, M.R., Goericke, R., Taylor, A.G., 2010. Modeling phytoplankton growth rates and chlorophyll to carbon ratios in California coastal and pelagic ecosystems. *Journal of Geophysical Research* 115, G04003. <http://dx.doi.org/10.1029/2009JC001111>.
- Lindo-Atchati, D., Bringas, F., Goni, G., 2013. Loop Current excursions and ring detachments during 1993–2009. *International Journal of Remote Sensing* 34 (14), 5042–5053. <http://dx.doi.org/10.1080/01431161.2013.787504>.
- Lipinski, D., Mohseni, K., 2014. Observations on the flow structures and transport in a simulated warm-core ring in the Gulf of Mexico. *Ocean Dynamics* 64 (1), 79–88.
- Liu, Y., Lee, S.-K., Muhling, B.A., Lamkin, J.T., Enfield, D.B., 2012. Significant reduction of the Loop Current in the 21st century and its impact on the Gulf of Mexico. *Journal of Geophysical Research*, 117. <http://dx.doi.org/10.1029/2011JC007555>, C05039.
- Luis, Capurro, R.A., Reid, Joseph L. (Eds.), 1972. *Contributions on the Physical Oceanography of the Gulf of Mexico*. volume 2 of Texas A & M University oceanographic studies, Texas A & M University Dept. of Oceanography. The University of California Press.
- Mahadevan, A., Tandon, A., Ferrari, R., 2010. Rapid changes in mixed layer stratification driven by submesoscale instabilities and winds. *Journal of Geophysical Research* 115, C03017. <http://dx.doi.org/10.1029/2008JC005203>.
- Mahadevan, A., D'Asaro, E., Lee, C., Perry, M.-J., 2012. Eddy-driven stratification initiates North Atlantic spring phytoplankton blooms, 2012. *Science* 337 (6090), 54–58. <http://dx.doi.org/10.1126/science.1218740>.
- Maltrud, M., Peacock, S., Visbeck, M., 2010. On the possible long-term fate of oil released in the Deepwater Horizon incident, estimated using ensembles of dye release simulations. *Environmental Research Letters* 5, 035301. <http://dx.doi.org/10.1088/1748-9326/5/3/035301>.
- Marshall, J., Adcroft, A., Hill, C., Perelman, L., Heisey, C., 1997a. A finite-volume, incompressible Navier-Stokes model for studies of the ocean on parallel computers. *Journal of Geophysical Research* 102 (C3), 5753–5766.
- Marshall, J., Hill, C., Perelman, L., Adcroft, A., 1997b. Hydrostatic, quasi-hydrostatic, and nonhydrostatic ocean modeling. *Journal of Geophysical Research* 102 (C3), 5733–5752.
- Martínez-López, B., Zavala-Hidalgo, J., 2009. Seasonal and interannual variability of cross-shelf transports of chlorophyll in the Gulf of Mexico. *Journal of Marine Systems* 77 (2009), 1–20. <http://dx.doi.org/10.1016/j.jmarsys.2008.10.002>.
- Maul, G.A., 1978. The 1972–1973 cycle of the Gulf Loop current. Part II: Mass and salt balances of the basin. *Symposium on Progress in Marine Research in the Caribbean and Adjacent Regions*. Caracas (Venezuela), 12 July 1976. FAO Fisheries Reports (FAO). No. 200 (suppl.), pp. 597–619.
- Maul, G.A., Mayer, D.A., Baig, S.R., 1985. Comparison between a continuous three-year current meter observation at the sill of the Yucatan Strait, satellite measurements of Gulf Loop Current area, and regional sea level. *Journal of Geophysical Research* 90, 9089–9096.

- Maul, G.A., Davis, A.M., Simmons, J.W., 2001. Seawater temperature trends at USA tide gauges. *Geophysical Research Letters* 28 (20), 3935–3937.
- McGillicuddy Jr., D.J., Johnson, R., Siegel, D.A., Michaels, A.F., Bates, N.R., Knap, A.H., 1999. Mesoscale variations of biochemical properties in the Sargasso Sea. *Journal of Geophysical Research* 104 (C6), 13381–13394. <http://dx.doi.org/10.1029/1999JC000021>.
- Melo Gonzalez, N., Muller-Karger, F.E., Cerdeira Estrada, S., Pérez de los Reyes, R., Victoria del Rio, I., Cárdenas Perez, P., Mitrani Arenal, I., 2000. Near-surface phytoplankton distribution in the western Intra-Americas Sea: The influence of El Niño and weather events. *Journal of Geophysical Research* 105 (C6), 14029–14043.
- Menemenlis, D., Fukumori, I., Lee, T., 2005a. Using greens functions to calibrate an ocean general circulation model. *Monthly Weather Review* 133, 1224–1240.
- Menemenlis, D., Hill, C., Adcroft, A., Campin, J., Cheng, B., Ciotti, B., Fukumori, I., Heimbach, P., Henze, C., Koehl, A., Lee, T., Stammer, D., Taft, J., Zhang, J., 2005b. NASA supercomputer improves prospects for ocean climate research. *Eos, Transactions American Geophysical Union* 86 (89), 95–96.
- Menemenlis, D., Campin, J., Heimbach, P., Hill, C., Lee, T., Nguyen, A., Schodlock, M., Zhang, H., 2008. ECCO2: high resolution global ocean and sea ice data synthesis. *Mercator Ocean Quarterly Newsletter* 31, 13–21.
- Menzel, D.W., Ryther, J.H., 1961. Annual variations in primary production of the Sargasso Sea off Bermuda. *Deep-Sea Research* 7, 282–288.
- Mildner, T.C., Eden, C., Czeschel, L., 2013. Revisiting the relationship between Loop Current rings and Florida current transport variability. *Journal of Geophysical Research: Oceans* 118, 1–10. <http://dx.doi.org/10.1002/2013JC009109>.
- Morel, A., Prieur, L., 1977. Analysis of variations in ocean color. *Limnology and Oceanography* 22, 709–722.
- Morey, S.L., Zavala-Hidalgo, J., O'Brien, J.J., 2005. The Seasonal variability of continental shelf circulation in the northern and Western Gulf of Mexico from a high-resolution numerical model. In: *Circulation in the Gulf of Mexico: Observations and Models*. Geophysical Monograph Series 161. American Geophysical Union, pp. 203–218. <http://dx.doi.org/10.1029/161GM16>.
- Morrison, Nowlin, W.D., 1977. Repeated nutrient, oxygen, and density sections through the Loop Current. *Journal of Marine Research* 35 (1), 105–128.
- Muhling, B.A., Lee, S.-K., Lamkin, J.T., Liu, Y., 2011. Predicting the effects of climate change on bluefin tuna (*Thunnus thynnus*) spawning habitat in the Gulf of Mexico. *ICES Journal of Marine Science* 68, 1051–1062.
- Muhling, B.A., Lamkin, J.T., Richards, W.J., 2012. Decadal-scale responses of larval fish assemblages to multiple ecosystem processes in the northern Gulf of Mexico. *Marine Ecology Progress Series* 450, 37–53. <http://dx.doi.org/10.3354/meps09540>.
- Muller-Karger, F.E., 1993. River discharge variability including satellite-observed plume-dispersal patterns. In: Maul, George (Ed.), *Climate Change in the Intra-Americas Sea*. United Nations Environmental Programme (Wider Caribbean Region) and Intergovernmental Oceanographic Commissions (Caribbean and Adjacent Regions). Edward Arnold Publishers, pp. 162–192 (Chapter 8).
- Muller-Karger, F.E., 2000. The spring 1998 NEGOM cold water event: remote sensing evidence for upwelling and for eastward advection of Mississippi Water (or: How an Errant LC Anticyclone Took the NEGOM for a Spin). *Gulf of Mexico Science* 1, 55–67.
- Muller-Karger, F.E., Walsh, J.J., Evans, R.H., Meyers, M.B., 1991. On the seasonal phytoplankton concentration and sea surface temperature cycles of the Gulf of Mexico as determined by satellites. *Journal of Geophysical Research* 96 (C7), 12645–12665.
- Muller-Karger, F.E., Kavanaugh, M.T., Montes, E., Balch, W.M., Breitbart, M., Chavez, F.P., Doney, S.C., Johns, E.M., Letelier, R.M., Lomas, M.W., Sosik, H.M., White, A.E., 2014. A Framework for a Marine Biodiversity Observing Network Within Changing Continental Shelf Seasapes. *Oceanography* 27 (2), 18–23. <http://dx.doi.org/10.5670/oceanog.2014.456>.
- NASA CZCS Technical Note, <http://oceancolor.gsfc.nasa.gov/ANALYSIS/PROTEST/c06m_sr2010.0m/comp Regional_rrs_mission.htm>, 2010. CZCS and SeaWiFS regional remote sensing reflectance trends..
- National Ocean Service, NOAA, <<http://stateofthecoast.noaa.gov>>, 2011. The Gulf of Mexico at a Glance: A Second Glance. Washington, DC: U.S. Department of Commerce.
- Nedbor-Gross, R., Dukhovskoy, D.S., Bourassa, M.A., Morey, S.M., Chassignet, E.P., 2014. Investigation of the relationship between the Yucatan Channel transport and the Loop Current area in a multidecadal numerical simulation. *Mar. Technol. Soc. J.* 48 (4), 15–26.
- Nof, D., 2005. The Momentum Imbalance Paradox Revisited. *Journal of Physical Oceanography* 35, 1928–1939.
- Nowlin, W.D., Hubertz, J., Reid, R., 1968. A detached eddy in the Gulf of Mexico. *Journal Marine Research* 26, 185–186.
- Nowlin, W.D. Jr., Jochens, A.E., DiMarco, S.F., Reid, R.O., 2000. Physical oceanography. In: Deepwater Gulf of Mexico Environmental and Socioeconomic Data Search and Synthesis. Narrative Report. OCS Study MMS 2000–049. Gulf of Mexico OCS Regional Office. Minerals Management Service. U.S. Department of the Interior, pp. 61–121 (Chapter 4).
- Oey, L.-Y., 1996. Simulation of mesoscale variability in the Gulf of Mexico: Sensitivity studies, comparison with observations, and trapped wave propagation. *Journal of Physical Oceanography* 26 (2), 145–175.
- O'Reilly, J.E., Maritorena, S., Siegel, D.A., O'Brien, M.C., Toole, D., Chavez, F.P., Strutton, P., Cota, G.F., Hooker, S.B., McClain, C.R., Carder, K.L., Muller-Karger, F.E., Harding, L., Magnuson, A., Phinney, D., Moore, G.F., Aiken, J., Arrigo, K.R., Letelier, R., Culver, M., 2000. In: Hooker, S.B., Firestone, E.R. (Eds.), *Ocean Chlorophyll-a Algorithms for SeaWiFS, OC2 and OC4: version 4*. SeaWiFS Postlaunch Calibration and Validation Analyses, Part 3. NASA Tech. Memo. 2000–206892, vol. 11. NASA Goddard Space Flight Center, Greenbelt, Maryland, pp. 9–23.
- Ortner, P.B., Lee, T.N., Milne, P.J., Zika, R.G., Clarke, M.E., Podesta, G.P., Swart, P.K., Tester, P.A., Atkinson, L.P., Johnson, W.R., 1995. Mississippi River flood waters that reached the Gulf Stream. *Journal of Geophysical Research* 100 (C7), 13595–13601. <http://dx.doi.org/10.1029/95JC01039>.
- Perez, R., Muller-Karger, F.E., Merino, M., Victoria, I., Melo, N., Cerdeira, S., 1999a. Cuban, Mexican, US researchers probing mysteries of Yucatan current. *Earth in Space* 12 (1), 10–14, September 1999.
- Perez, R., Muller-Karger, F.E., Victoria, I., Melo, N., Cerdeira, S., 1999b. Cuban, Mexican, US researchers probing mysteries of Yucatan current. *EOS, AGU Transactions* 80 (14), 153.
- Piontkovski, S., Nezlin, N., 2012. Mesoscale eddies of arabian Sea: physical-biological interactions. *International Journal of Marine Science* 2 (7), 51–56. <http://dx.doi.org/10.5376/ijms.2012.02.0007>.
- Platt, T., Fuentes-Yaco, C., Frank, K.T., 2003. Spring algal bloom and larval fish survival. *Nature* 423.
- Platt, T., Sathyendranath, S., Fuentes-Yaco, C., 2007. Biological oceanography and fisheries management: perspective after 10 years. *Ices Journal of Marine Science* 64 (5), 863–869.
- Poore, R.Z., DeLong, K., Richey, J., Quinn, T.M., 2009. Evidence of multidecadal climate variability and the Atlantic multidecadal oscillation from a Gulf of Mexico sea-surface temperature-proxy record. *Geo-Marine Letters* 29 (6), 477–484.
- Rio, M.-H., Hernandez, F., 2004. A mean dynamic topography computed over the world ocean from altimetry, in situ measurements, and a geoid model. *Journal of Geophysical Research* 109, C12032. <http://dx.doi.org/10.1029/2003JC002226>.
- Rivas, D., Badan, A., Ochoa, J., 2005. The ventilation of the deep Gulf of Mexico. *Journal of physical oceanography* 35, 1763–1781.
- Roemmich, D., Gould, W.J., Gilson, J., 2012. 135 years of global ocean warming between the Challenger expedition and the Argo Programme. *Nature Climate Change*. <http://dx.doi.org/10.1038/nclimate1461>.
- Ryther, J.H., Menzel, D.W., 1960. The seasonal and geographical range of primary production in the Western Sargasso Sea. *Deep-Sea Research* 6, 235–238.
- Salisbury, J.E., Campbell, J.W., Linder, E., Meeker, L.D., Muller-Karger, F.E., Vorosmarty, C.J., 2004. On the seasonal correlation of particle fields with wind stress and Mississippi discharge in the northern Gulf of Mexico. *Deep-Sea Research II* 51, 1187–1203.
- Salmerón-García, O., Zavala-Hidalgo, J., Mateos-Jasso, A., Romero-Centeno, R., 2011. Regionalization of the Gulf of Mexico from space-time chlorophyll-a concentration variability. *Ocean Dynamics* 61, 439–448. <http://dx.doi.org/10.1007/s10236-010-0368-1>.
- Sangrà, P., Pascual, A., Rodríguez-Santana, Á., Machín, F., Mason, E., McWilliams, J.C., Pelegri, J.L., Dong, C., Rubio, A., Aristegui, J., Marrero-Díaz, Á., Hernández-Guerra, A., Martínez-Marrero, A., Auladell, M., 2009. The canary eddy corridor: a major pathway for long-lived eddies in the subtropical North Atlantic. *Deep-Sea Research* 56 (2009), 2100–2114.
- Scranton, M.I., Taylor, G.T., Thunell, R., Benitez-Nelson, C.R., Muller-Karger, F., Fanning, K., Lorenzoni, L., Montes, E., Varela, R., Astor, Y., 2014. Interannual and subdecadal variability in the nutrient geochemistry of the Cariaco Basin. *Oceanography* 27 (1).
- Shay, L.K., Goni, G.J., Black, P.G., 2000. Effects of a warm oceanic feature on hurricane Opal. *Monthly Weather Review* 128, 1366–1383.
- Sheinbaum, J., Candela, J., Badan, A., Ochoa, J., 2002. Flow structure and transport in the Yucatan Channel. *Geophysical Research Letters* 29 (3). <http://dx.doi.org/10.1029/2001GL013990>.
- Shi, C., Nof, D., 1994. The destruction of lenses and generation of wodons. *Journal of Physical Oceanography* 24 (6), 1120–1136.
- Siegel, D.A., Behrenfeld, M.J., Maritorena, S., McClain, C.R., Antoine, D., Bailey, S.W., Bontempi, P.S., Boss, E.S., Dierssen, H.M., Doney, S.C., Eplee Jr., R.E., Evans, R.H., Feldman, G.C., Fields, E., Franz, B.A., Kuring, N.A., Mengelt, C., Nelson, N.B., Patt, F.S., Robinson, W.D., Sarmiento, J.L., Swan, C.M., Werdell, P.J., Westberry, T.K., Wilding, J.G., Yoder, J.A., 2013. Regional to global assessments of phytoplankton dynamics from the SeaWiFS mission. *Remote Sensing of Environment* 135, 77–91. <http://dx.doi.org/10.1016/j.rse.2013.03.025>.
- Sturges, W., Leben, R., 2000. Frequency of ring separations from the loop current in the Gulf of Mexico: a revised estimate. *Journal of Physical Oceanography* 30 (7), 1814–1819.
- Sverdrup, H.U.J., 1953. On conditions for the vernal blooming of phytoplankton. *Conseil Perman. Int. Explor. Mer.* 18, 287–295.
- Tang, W., Liu, W.T., Stiles, B., Fore, A., 2014. Detection of diurnal cycle of ocean surface wind from space-based observations. *International Journal of Remote Sensing* 35 (14), 5328–5341. <http://dx.doi.org/10.1080/01431161.2014.926413>.
- Trenberth, K.E., Jones, P.D., Ambenje, P., Bojariu, R., Easterling, D., Klein Tank, A., Parker, D., Rahimzadeh, F., Renwick, J.A., Rusticucci, M., Soden, B., Zhai, P., 2007. Observations: surface and atmospheric climate change. In: Solomon, S., Qin, D., Manning, M., Chen, Z., Marquis, M., Averyt, K.B., Tignor, M., Miller, H.L. (Eds.), *Climate Change 2007: The Physical Science Basis. Contribution of Working Group I to the Fourth Assessment Report of the Intergovernmental Panel on Climate Change*. Cambridge University Press, Cambridge, United Kingdom and New York, NY, USA, pp. 235–336.
- Tulloch, R.R., Hill, C.C., Jahn, O.O., 2011. Possible spreadings of buoyant plumes and local coastline sensitivities using flow syntheses from 1992 to 2007. *Monitoring and Modeling the Deepwater Horizon Oil Spill: A Record-Breaking Enterprise*, 245–255.

- Twilley, R.R., Barron, E.J., Gholz, H.L., Harwell, M.A., Miller, R.L., Reed, D.J., Rose, J.B., Sieman, E.H., Wetzel, R.G., Zimmerman, R.J., 2001. Confronting climate change in the Gulf coast region: Prospects for sustaining our ecological heritage. In: Union of Concerned Scientists, Cambridge, Massachusetts, and Ecological Society of America, Washington, DC, p. 82.
- Vidal, V.M.V., Vidal, F.V., Hernández, A.F., Meza, E., Zambrano, L., 1994. Winter water mass distributions in the Western Gulf of Mexico affected by a colliding anticyclonic ring. *Journal of Oceanography* 50, 559–588.
- Villanueva, E.E., Mendoza, V.M., Adem, J., 2010. Sea surface temperature and mixed layer depth changes due to cold-air outbreak in the Gulf of México. *Atmósfera* 23 (4), 325–346.
- Vukovich, F.M., 1988. Loop current boundary variations. *Journal of Geophysical Research* 93 (C12), 15585–15591.
- Vukovich, F.M., 2007. Climatology of ocean features in the Gulf of Mexico using satellite remote sensing data. *Journal of Physical Oceanography* 37 (3), 689–707.
- Vukovich, F.M., 2012. Changes in the loop current's eddy shedding 854 in the period 2001–2010. *Int. J. Oceanogr.*, 18 <http://dx.doi.org/10.1155/2012/439042>. Article ID 439042.
- Vukovich, F.M., Crissman, B.M., Bushnell, M., King, W.J., 1979. Some aspects of the oceanography of the Gulf of Mexico using satellite and in situ data. *Journal of Geophysical Research* 84 (C12), 7749–7768.
- Wahl, Thomas, Calafat, Francisco M., Luther, Mark E., 2014. Rapid changes in the seasonal sea level cycle along the US Gulf coast from the late 20th century. *Geophysical Research Letters* 41. <http://dx.doi.org/10.1002/2013GL058777>.
- Weisberg, R.H., Black, B.D., Yang, H., 1996. Seasonal modulation of the West Florida continental shelf circulation. *Geophysical Research Letters* 23 (17), 2247–2250. <http://dx.doi.org/10.1029/96GL02184>.
- Weisberg, R.H., He, R., Kirkpatrick, G., Muller-Karger, F., Walsh, J.J., 2004. Coastal ocean circulation influences on remotely sensed optical properties: a West Florida shelf case study. *Oceanography* 17, 68–75.
- Weisberg, R.H., He, R., Liu, Y., Virmani, J.I., 2005. West Florida shelf circulation on synoptic, seasonal, and inter-annual time scales. In: Sturges, W., Lugo-Fernandez, A. (Eds.), *Circulation in the Gulf of Mexico*. AGU monograph series, Geophysical Monograph, pp. 325–347.
- Willis, J.K., Roemmich, D., Cornuelle, B., 2004. Interannual variability in upper ocean heat content, temperature, and thermosteric expansion on global scales. *Journal of Geophysical Research* 109, C12036. <http://dx.doi.org/10.1029/2003JC002260>.
- Wolter, K., Timlin, M.S., 2011. El Niño/Southern Oscillation behaviour since 1871 as diagnosed in an extended multivariate ENSO index (MEI.ext). *Intl. J. Climatol.* 31 (7), 14. <http://dx.doi.org/10.1002/joc.2336>.
- Wunsch, C., Heimbach, P., Ponte, R., Fukumori, I., 2009. The global general circulation of the ocean estimated by the ECCO-consortium. *Oceanography* 22, 88–103.
- Yoder, J.A., 1979. Effect of temperature on light-limited growth and chemical composition of *Skeletonema costatum* (Bacillariophyceae). *Journal of Phycology* 15, 362–370.
- Young, I.R., Zieger, S., Babanin, A.V., 2011a. Global trends in wind speed and wave height. *Science* 332 (6028), 451–455. <http://dx.doi.org/10.1126/science.1197219>.
- Young, I.R., Babanin, A.V., Zieger, S., 2011b. Response to comment on “Global Trends in Wind Speed and Wave Height”. *Science* 905. <http://dx.doi.org/10.1126/science.1210548>.
- Zavala-Hidalgo, J., Morey, S.L., O'Brien, J.J., 2003. Seasonal circulation on the western shelf of the Gulf of Mexico using a high-resolution numerical model. *Journal of Geophysical Research* 108 (C12), 3389. <http://dx.doi.org/10.1029/2003JC001879>.
- Zavala-Hidalgo, J., Morey, S.L., O'Brien, J.J., Zambudio, L., 2006. On the loop current eddy shedding variability. *Atmósfera* 19 (1), 41–48.